



Available online at www.sciencedirect.com

ScienceDirect

Geochimica et Cosmochimica Acta 285 (2020) 150-174

Geochimica et Cosmochimica Acta

www.elsevier.com/locate/gca

Revisiting water speciation in hydrous alumino-silicate glasses: A discrepancy between solid-state ¹H NMR and NIR spectroscopy in the determination of X-OH and H₂O

George D. Cody ^{a,*}, Michael Ackerson ^{a,b}, Carolyn Beaumont ^a, Dionysis Foustoukos ^a, Charles Le Losq ^{a,c}, Bjorn O. Mysen ^a

^a Earth and Planets Laboratory, Carnegie Institution for Science, 5251 Broad Branch Rd., NW, Washington, DC, United States

^b Museum of Natural History, Smithsonian Institution, United States

^c College of Science, Australian National University, Australia

Received 15 July 2019; accepted in revised form 6 July 2020; Available online 15 July 2020

Abstract

The speciation of water dissolved into and reacted with hydrous alumino-silicate glasses (of NaAlSi₃O₈ and "rhyolitic" compositions) quenched from high temperature is re-investigated where the predominant species are expected to be "X(Si and Al)-OH" and "H₂O". Only, two analytical methods are capable of assessing such speciation: Near InfraRed (NIR) spectroscopy and solid-state ¹H Nuclear Magnetic Resonance (NMR) spectroscopy. It is observed that the apparent water speciation, as a function of total water content, as determined by NIR spectroscopy is nearly the opposite from what the 1H NMR data reveal. Deuterium (²H) NMR and silicon (²⁹Si) NMR report consistent trends in apparent speciation (depolymerization) with those indicated by the ¹H NMR data. Compared with four previous NMR studies of hydrous NaAlSi₃O₈ glasses it is shown that whereas NIR data always report the same apparent systematic variation in the intensity of the 4500 ("X-OH") and 5200 ("H₂O") cm⁻¹ bands with total water content, multiple ¹H NMR studies of hydrous NaAlSi₃O₈ report a wide range in OH/H₂O. The discrepancy between the various NMR studies likely reflects differences in how the various glasses were made. Specifically, quench rate (fast or slow) and synthesis pressure (higher or lower), might impose a strong effect on observed water speciation in glasses via ¹H NMR. It is concluded that the application of NIR spectroscopy, specifically the use of the intensities of the 4500 ("X-OH") and 5200 ("H₂O") cm⁻¹ NIR bands, does not provide an accurate assessment of water speciation in hydrous alumino-silicate glasses. NIR spectroscopy does remain a very valuable analytical tool for determination of total water content. © 2020 Published by Elsevier Ltd.

Keywords: Water speciation; Hydrous glasses; 1H NMR; Near IR spectroscopy

1. INTRODUCTION AND BACKGROUND

In principle, water is expected to dissolve into an aluminosilicate melt either as molecular H₂O or it may react (depolymerize) with Si—O—Si (or Si—O—Al) linkages to form

X(Si or Al)-OH species (written as an equilibrium in Eq. (1)).

$$(OR)_3Si-O-Si(OR)_3 + H_2O = 2 (OR)_3Si-OH R = Si, Al, or H$$
 (1)

It is noted that in the case of hydrous peralkaline glasses with large initial NBO/T's (where NBO refers to the number of Non Bridging Oxygens, oxygens not bonded to either

^{*} Corresponding author.

E-mail address: gcody@ciw.edu (G.D. Cody).

 ${\rm Si}^{4+}$ or ${\rm Al}^{3+}$ in either silica or alumina tetrahedral, and T refers to the number of "tetrahedra") an additional solution mechanism has been proposed where in ${\rm M(OH)_{1-2}}$ species (M = alkali and alkaline earth elements) may also form (Xue and Kanzaki, 2004; Cody et al., 2005) and that reduces the degree of depolymerization by addition of water. At low NBO/T_{DRY} compositions, e.g. NaAlSi₃O₈ glasses, this later solution mechanism has not been observed and is not expected (Xue and Kanzaki, 2004, 2008).

It is certainly to be expected that nature of water speciation (Eq. (1)), hence melt depolymerization, in hydrous melts will play an important role in melt properties. The degree of melt depolymerization, quantified by NBO/T, has a well-established and profound effect on a wide variety of melt properties (see review by Mysen and Richet, 2019). For example, the viscosity of anhydrous melts is well known to drop by orders of magnitude with increased NBO/T (e.g., Urbain et al., 1982, Knoche et al., 1994, Giordano and Dingwell, 2003, a broad review this subject is available in Mysen and Richet, 2019). Similarly, electrical conductivity in anhydrous silicate melts increases by orders of magnitude with increasing NBO/T (Tickle, 1967). The degree of melt depolymerization has also been shown to influence compositional factors such as noble gas solubility [solubility drops with increasing NBO/T, Carrol and Stolper (1993)] and element partitioning between melts and crystals [e.g. K_D^{Mg} between melt and olivine crystals drops precipitously with increasing NBO/T, Kushiro and Mysen (2002), whereas K_D^{Mn} between melt and olivine crystals increases with increased NBO/T, Mysen (2007)]. In the case of noble gas solubility the effect of NBO/T is interpreted to result from a reduction in "ionic porosity" (Carrol and Stolper, 1993), whether "ionic porosity" is responsible for the reduction in K_D^{Mg} between olivine and melts as a function of NBO/T is not certain.

Given that H₂O can act as both like an inert volatile species (like Ar or Xe) or as a network modifying component (like Na₂O) means that understanding the extent which role H₂O plays is very important. Phenomenologically, the addition of water has a very strong effect on melt properties, as significant as increases in NBO/T for anhydrous melts. For example, with the addition of water melt viscosity can be reduced by many orders of magnitude (e.g. Shaw, 1963; Burnham, 1963; Richet et al., 1996; Whittingston et al., 2001; Romano et al., 2001; Poe et al., 2006 and others). Similarly, the addition of water to anhydrous silicate melts significantly (by orders of magnitude) increases electrical conductivity (e.g. Ni et al., 2011; Guo et al., 2016). In general, the effect of addition of water to a given anhydrous silicate melt appears very similar in magnitude to the effect of increasing NBO/T with anhydrous silicate melts (see references above). These significant responses due to the addition of water could imply that that the primary effect of water addition is an increase in NBO/T (Eq. (1)).

The crux of the problem is quantifying the speciation of water (Eq. (1)) in melts and glasses. There are only two regions in the electromagnetic spectrum that potentially could provide a direct molecular spectroscopic detection, and possibly discrimination and quantification, of X-OH

and H_2O species in solids such as minerals and glasses. These are; (i) in the infrared (IR) region O—H fundamental vibrational (stretching) bands are strong and (ii) in the radio frequency range nuclear spin transitions of 1H nuclei (spin I = $^1\!/_2$) and D (2H) nuclei (spin I = 1) provide a spectroscopic window into H molecular speciation. In some cases, e.g. alkali silicate glasses, the application of 29 Si NMR can indirectly enable assessment of X-OH content through revealing changes in the number of silica tetrahedra with non-bridging oxygens (NBOs) that form upon reaction with water, Eq. (1) (e.g. Kummerlen et al., 1992, Zotov and Keppler, 1998, Robert et al., 2001, Xue and Kanzaki, 2004, Cody et al., 2005, Le Losq et al., 2015b, Wang et al., 2015).

While both IR and ¹H-, and D-NMR spectroscopies are very sensitive to detecting hydrogen (or D) bearing molecules and can be used to quantitate total H(D) abundance in solids (e.g. Eckert et al., 1988), none of these spectroscopies can discriminate between X-OH and H₂O species based on primary molecular spectroscopic behavior, e.g. the fundamental vibrational mode frequencies (IR) or the chemical shift (H and D-NMR). Rather, indirect methods have to be employed, that in both cases (IR and NMR) add potential uncertainty to the speciation analysis.

In the case of IR spectroscopy, the frequencies of the fundamental vibrational stretching modes for both X-OH and H₂O species in hydrous glasses are primarily (if not entirely) controlled by O—H bond lengths, where such variation is typically due to variation in the strength of hydrogen bonding (Hammer et al., 1998; Libowitsky, 1999). Hydrogen in both H₂O and X-OH species can experience equal variation in H-bonding interactions and O-H bond lengths, thus there potentially exists unresolvable overlap in the X-OH and H₂O fundamental stretching frequencies over a wide range of the Mid IR region. This negates the guaranteed possibility of quantitative determination of the distribution of hydrogen into X-OH and H₂O species in silicate glasses through analysis of the fundamental O-H vibrational modes.

The problem of differentiating X-OH and H₂O was apparently resolved when it was proposed (Scholtz, 1960) that certain very weak absorption features that are apparent in the near IR (NIR) region (frequencies > 3800 cm⁻¹) could be attributed to combination bands arising from the addition of low frequency bending modes (at \sim 1000 cm⁻¹ and 1600 cm⁻¹, for X-OH and H₂O, respectively) with fundamental OH stretching modes (2800-3600 cm⁻¹, for both X-OH and H₂O) yielding a purely X-OH combination band at ~4500 cm⁻¹ and a purely H_2O combination band at $\sim 5200 \text{ cm}^{-1}$ (Scholtz, 1960, Bartholomew et al., 1980). It has repeatedly been shown in many studies of variably hydrated silicate glasses that the intensities of these two NIR bands vary systematically and reproducibly with water content of glasses over a wide range of compositions. This was first done in an early study of hydrous Na-K-Al-Zn silicate glasses (Bartholomew et al., 1980) and later expanding to hydrous rhyolite glasses (Stolper, 1982, Newman et al., 1986, Silver and Stolper, 1989, Silver et al., 1990), "albitic" (NaAlSi₃O₈) glasses (Silver and Stolper, 1989, Silver et al., 1990, Schmidt

et al., 2001 and others), "orthoclase" (KAlSi₃O₈) glasses (Silver et al., 1990, Schmidt et al., 2001), calcium aluminosilicate glasses (Silver et al., 1990), peralkaline aluminosilicate glasses (Behrens et al., 1996), Jadeite and nepheline composition glasses (Malfait and Xue, 2010) and as well as simple hydrous peralkaline glasses, e.g., sodium silicate glasses (Takata et al., 1981, Acocella et al., 1984, Zotov and Keppler, 1998, Yamashita et al., 2008, Le losq et al., 2015a), and other hydrous alkali silicate glasses (lithium and potassium tetrasilicate glasses, Le losq et al., 2015a).

Analysis of changes in intensity of the NIR bands in glasses of all compositions consistently indicates that with increasing total water content the intensity of the combination band ascribed to X-OH species (4500 cm⁻¹) initially increases faster than the NIR band assigned to H₂O species (5200 cm⁻¹), but quickly plateaus to a constant or even slightly decreasing intensity at higher water concentrations. The NIR band ascribed to H₂O species, on the other hand, increases continuously with increasing total water content. Therefore, the NIR studies reveal a cross over in the apparent X-OH and H₂O speciation with increasing total water content; this cross over point ranges from \sim 3 up to 6 wt % for aluminosilicate and sodium tetrasilicate glasses, respectively, measured at room temperature (Stolper, 1982, Silver and Stolper, 1989, Silver et al., 1990, Zotov and Keppler, 1998). It has also been shown that the NIR spectral features evolve with increasing temperatures above the glass transition, such that at high temperatures, for a given water composition, the 4500 cm⁻¹ peak becomes more intense than the 5200 cm⁻¹ band suggesting that X-OH concentration becomes dominant at any water concentration as temperature increases (e.g. Stolper, 1989, Nowak and Behrens, 1995, Shen and Keppler, 1995; Sowerby and Keppler, 1999, Nowak and Behrens, 2001, Cherikova and Yamashita, 2015).

There has been comparably less application of solid state ¹H NMR to the analysis of water speciation in silicate glasses. Fundamentally, ¹H solid state NMR suffers from the same issues that confront IR, i.e., the primary observable in ¹H NMR, the chemical shift, is controlled primarily by the strength of hydrogen bonding and resulting O-H bond length (Eckert et al., 1988, Xue and Kanzaki, 2004). As is the case in IR spectroscopy, with ¹H NMR both X-OH and H₂O can experience equal variation in hydrogen bonding strengths. Overlap of Si-OH and H₂O signals is, therefore, expected and experimentally confirmed through dipolar dephasing studies by Robert et al. (2001) and Xue and Kanzaki (2004). Unlike the proposed NIR combination bands, however, there are no regions in the ¹H NMR spectrum where X-OH and H₂O species can be uniquely distinguished by frequency. In the case hydrous aluminosilicate glasses Malfait and Xue (2010) did identify a low frequency peak/shoulder via ¹H NMR that systematically increased in intensity as the Al/Si + Al ratio increased. Through ²⁷Al-¹H cross polarization NMR it was shown that the ¹H corresponding to this peak/shoulder is in close proximity to ²⁷Al. Malfait and Xue (2010) concluded based on the low water content (<1wt%) and NIR measurements that water speciation must be predominantly X-OH and the low frequency peak is, therefore, Al-OH, however this assignment is inferred not proven.

There is a physical interaction that manifests a significant effect on the ¹H solid state NMR spectrum that is not complementary with any IR observables. This is the magnetic interaction between neighboring hydrogen atoms, physically described as dipolar coupling (Abragam, 1961). In principle, it is relatively straightforward to use the dipolar coupling interaction to distinguish X-OH and H₂O species (Bartholomew and Schreurs, 1980, Eckert et al., 1988, Zavelisky et al., 1999, Riemer et al., 2001, Schmidt et al., 2001, Yamashita et al., 2008), Hydrogen atoms in H₂O will always be close enough to induce detectible signal of dipolar coupling. However, in the case of isolated (Si,Al)-OH's, hydrogen-hydrogen distances probably will be too far apart to experience significant dipolar coupling. Thus, there have been a number of NMR studies of hydrated silicate glasses where the intensity of dipolar interactions in ¹H solid state NMR spectra has been used to ascertain the relative abundances of H₂O and (Si,Al)-OH species: these include static ¹H NMR (Bartholomew and Schreurs, 1980, Eckert et al., 1988, Zavelisky et al., 1999, Riemer et al., 2001, Schmidt et al., 2001, Yamashita et al, 2008) and with Magic Angle Spinning (MAS) (Eckert et al., 1988, Kohn et al., 1989); and also with deuterium (D or ²H) NMR (Eckert et al., 1987). In some cases ¹H NMR reports the same X-OH and H₂O speciation as predicted by near IR measurement of hydrous alumino-silicate glasses (Schmidt et al., 2001), but in other cases speciation derived from ¹H NMR deviates from the near IR data predictions (e.g. Eckert et al., 1988). Yamashita et al. (2008) noted in their study of hydrous peralkaline silicate glasses that there was a significant discrepancy in water speciation between that determined in their static ¹H HMR spectra and NIR spectra of the same glasses.

The disparity between ¹H NMR and NIR results has led to reinvestigation of the use of MAS ¹H NMR to ascertain X-OH and H₂O speciation on a well-studied glass composition (hydrous NaAlSi₃O₈ glasses quenched from melts). The results of solid state ¹H NMR spectroscopy with moderately fast MAS (relative to previous studies) are used the measure the magnitude of proton dipolar coupling (as was first done by Eckert et al., 1988) in variously hydrated NaAlSi₃O₈ and model rhyolite glasses to estimate the speciation of H₂O and Si,Al-OH as a function of water content. In a more limited way D MAS NMR and ²⁹Si MAS NMR were used to test for internal consistency with the results derived from ¹H MAS NMR. NIR spectroscopic data on the same hydrous glasses were acquired for comparison with the NMR studies.

2. EXPERIMENTAL

2.1. Glass synthesis

The NaAlSi₃O₈ glasses were synthesized by mixing spectroscopically pure anhydrous SiO₂, Al₂O₃, and Na₂CO₃ powders followed by grinding in ethanol for at least one hour. After drying, the mixtures placed in a platinum crucible and were slowly heated up to 1400 °C in an

atmospheric pressure vertical tube furnace (DelTech). After a period of time the melt was quenched by placing the bottom of the crucible in liquid water. The dry starting material was reground in ethanol for ca. 1 hour and then placed in an oven at 400 °C to remove all ethanol and then stored at 110 °C in a drying oven to avoid any reaction with atmospheric water vapor. The composition of the starting glass was verified using a X-ray fluorescence spectrometer (Spectro XEPOS XRF).

The synthesis of hydrous melts was performed by melting the starting glass with measured amounts of H₂O at high pressure using a piston cylinder apparatus (Boyd and England, 1960). Each sample was loaded into a \sim 10 mm long, 5 mm diameter platinum capsule that is initially weighed empty. The following protocol is employed. First a measured amount of water is added to the capsule using a precision syringe followed by the capsule being reweighed. Next the appropriate mass of anhydrous glass (to achieve the desired degree of hydration) is loaded and the capsules are weighed again. The capsule top is then cut and reweighed. Finally, welding is performed using a pulsed arc welder (PUK Pro model 3S) with care taken to avoid any heating of the capsule. The final capsule weight after welding is measured to ensure no loss of water occurred during welding. The welded capsules were placed into ³/₄ inch diameter furnace assemblies (Kushiro, 1976), loaded into the piston cylinder apparatus and pressurized to 1.5 GPa and heated to 1400 °C (where temperature is measured with an S type thermocouple) for 2 hours. Upon switching off power to the furnace, the samples quench at a rate of approximately 100 °C/sec. Ten samples with NaAlSi₃O₈ composition and nominal water contents of 1-10 wt% water were synthesized (Table 1). The measured water contents compare favorably with the nominal water content as determined by recorded mass, measured ¹H NMR signal intensity per sample mass (calibrated with a known H-bearing standard), and hydrogen yield per sample mass determined with an elemental analyzer coupled to an isotope ratio mass spectrometer (Table 1). After each experiment, all samples were stored in their welded capsules until solid state NMR analysis was performed to minimize any hydration/dehydration of the glasses.

A second set of glasses, here on referred to as "Felsic Glass" (FG), were synthesized having a composition of a model rhyolite (in mol %: 80 % SiO₂, 10 % Al₂O₃, 3.33 % Na₂O, 3.34 % K₂O, 0.8 % MgO, 1.87 % CaO, and 0.67 % Fe₂O₃). This composition was designed to be an average for calc-alkaline rhyolites typical of the Western US. The synthesis of hydrated glasses from this starting composition was performed identically to that of the hydrated NaAlSi₃-O₈ compositions. Beyond the addition of small amounts of alkaline Earth elements and a slightly larger Si/Al ratio, the most notable difference in comparison with the NaAlSi₃O₈ composition glasses is the presence of iron. X-ray fluorescence analysis of the starting glass revealed that the iron concentration after melting and quenching is actually 0.3 mol % (by X-ray fluorescence) indicating loss of iron to the platinum capsule. The presence of paramagnetic iron is expected to have an effect on ¹H NMR spectra (Eckert et al., 1988) and may inhibit the ability to distinguish hydrogen-hydrogen coupling interactions from Fe (e⁻)-hydrogen coupling interactions. The possible effects of such interactions will be addressed further in the discussion.

For the purpose of collecting D MAS NMR spectra for comparison with 1H MAS NMR spectra, a limited series of deuterated NaAlSi $_3O_8$ glasses were synthesized with D $_2O$ at molar concentration equal to the molar abundance of H $_2O$ at 5, 6, and 7 wt%. Deuterated samples of lithium, sodium and potassium tetrasilicate (XS4, X = Li $_2O$, Na $_2O$, K $_2O$) glasses were also synthesized with 17.6 mol 9 0 D $_2O$ 0 (\sim 6 wt% total water).

2.2. FTIR Analysis

Infra-red spectroscopy of the variously hydrated NaAlSi $_3$ O $_8$ glasses was performed using doubly polished glass disks ca $80\text{--}100\,\mu\text{m}$ thick and analyzed using a Jasco IMV-4000 multichannel Fourier Transform Infra Red spectrometer/microscope with a liquid nitrogen cooled MCT detector. Typically 1000 interferograms were acquired at a resolution of 4 cm $^{-1}$ and co-added to provide sufficient resolution of the NIR bands. No effort was made to determine glass density and extinction coefficients for the purpose of an absolute determination of "X-OH" and "H $_2$ O" concentrations.

2.3. NMR spectroscopy

All Solid State Nuclear Magnetic Resonance (NMR) Spectroscopy experiments were performed at the W. M. Keck Solid State NMR Facility at the Earth and Planets Laboratory of the Carnegie Institution for Science. This lab employs a Chemagnetics Infinity solid state NMR multichannel spectrometer based around a 7.05 Tesla superconducting solenoid magnet. The frequency of ¹H at this field strength is on the order of 300 MHz. All ¹H solid state NMR spectra were acquired using a 2.5 mm OD magic angle spinning (MAS) double resonance (¹H-X) RF probe. Excitation pulses ($\pi/2 = 90$ ° nutation) were 2.5 µs in duration. A background suppression routine (DEPTH) was employed to suppress background ¹H signal from spins outside of the sample coil, that experience an effective pulse tip angle of <45°. In each case the sample spinning frequency for MAS $(\omega_r/2\pi)$ was 22 KHz (with a measured drift of less than ± 20 Hz). In each case the number of acquisitions was 8000 and the recycle delay was 10 seconds. The spectra are normalized in frequency to the ¹H resonance in tetramethylsilane (TMS), defined as 0 ppm relative to the carrier frequency.

In a few cases $D(^2H)$ solid-state NMR spectra were acquired using a 5 mm OD double resonance probe where the resonant frequency of 2H at \sim 7 Tesla is 46.1 MHz. The spectral width was 500 KHz and magic angle sample spinning was performed at 8 KHz (\pm 1 Hz). Excitation pulses (corresponding to a 10 ° nutation angle) were 0.5 μ s. In each case, 34,000 FID's were acquired and the recycle delay was 5 seconds, the spectra were referenced to TMS-D.

A limited number of ²⁹Si solid state NMR data were also acquired for the Fe containing "FG" glasses (where

Table 1 Water contents in hydrous Albite (NaAlSi₃O₈) composition glasses and NIR and ¹H NMR data.

Nominal water content (wt%)	Weighed water content (wt%) ^a	H NMR determined water content (wt%) ^b	IRMS determined water content (wt%) ^c	A_{4500}^{d}	$A_{5200}^{}$	Thickness (mm) ^f	$\Sigma SB(1)/CB^g$	uncertainty ^h	OH ⁱ Mol %	H ₂ O ^j Mol %
0	0	0	0	0.00	0.00	0.000	0.000	_	0.00	0.00
1	0.8	0.4	1.1 ± 0.04	3.28	0.80	0.111	0.087	± 0.003	1.77	1.77
2	1.7	1.1	1.1 ± 0.04	3.51	0.71	0.098	0.112	± 0.005	2.07	4.84
3	2.6	3.0	3.0 ± 0.10	6.74	5.74	0.083	0.116	± 0.003	3.64	6.47
4	3.9	4.3	4.1 ± 0.14	5.67	6.85	0.087	0.128	± 0.002	3.82	9.34
5	4.8	4.4	5.0 ± 0.17	6.37	11.73	0.094	0.115	± 0.002	5.63	10.45
6	5.9	5.8	5.0 ± 0.13	6.85	11.13	0.082	0.109	± 0.002	7.16	11.69
7	6.9	8.4	6.3 ± 0.17	6.36	17.58	0.098	0.092	± 0.002	10.10	11.39
8	7.9	7.4	7.2 ± 0.20	_	_	_	0.075	± 0.002	12.74	10.34
10	9.8	-	8.9 ± 0.24	_	_	_	0.048	± 0.002	20.73	8.06

Water as weighed into platinum capsule.
 Water content as compared with ¹H NMR signal intensity of gypsum standard.

^c Water detected upon heating in Isotope Ratio Mass Spectrometer (ave of duplicate)

d Integrated area of the 4500 cm⁻¹ peak

e Integrated area of the 5200 cm⁻¹ peak

f Measured thickness (mm) of glass wafers for NIR analysis.

g Sum of integrated $n \pm 1$ spinning bands divided by the integral of the center band h Based on center band and side band signal to noise ratios (SNR)

i Mol % of X (Si,Al) – OH groups relative to molar abundance of total water j Mol % of H₂O molecules relative to molar abundance of total water.

the presence of Fe significantly reduces 29 Si T_1 relaxation providing reasonable signal to noise (S/N) 29 Si NMR spectra without inordinate amounts of time or sample). A 5 mm double resonance probe tuned to the resonant frequency of 29 Si at 59.6 MHz was used. These single pulse experiments employed a pulse width of 1.3 μ s (corresponding to a 30 $^{\circ}$ nutation angle), a recycle delay of 2 s (Maekawa et al., 1991), and 39,000 acquisitions. The spectra were referenced to TMS.

NMR simulations were performed using the SIMPSON program that performs simulation of solid-state NMR experiments (Bak et al., 2000). The SIMPSON program efficiently solves the time evolution of the spin density matrix accounting for all internal interactions (e.g., the chemical shift, dipolar, and quadrupolar Hamiltonians) and external interactions (external magnetic field and RF pulses, power and duration) for randomly oriented solids (powders) as specified by the user.

2.4. Elemental analysis

The elemental hydrogen analyses were performed with a Thermo Finnigan Delta Plus XL mass spectrometer connected to a Thermo Finnigan Thermal Conversion elemental analyzer (TC/EA) operating at 1400 °C. H₂ reference gas of known δD composition (-123.39 % SMOW). International standards were used to calibrate and correct the data; internal working gas standards were analyzed at regular intervals to monitor the accuracy of the measured isotopic ratios and elemental compositions throughout the run. House standards, have been calibrated against international (SMOW, NBS-22, air) and commercially certified standards from Isoanalytical, USGS, NBS and Oztech. An H₃⁺ correction was determined and applied to the hydrogen measurements. Reported uncertainties on the elemental and isotopic analysis correspond to a 1 σ deviation between replicate analyses of distinct subsamples (n > 2).

3. RESULTS

3.1. NIR Spectroscopy

The NIR spectral regions for the hydrated NaAlSi₃O₈ glasses are presented in Fig. 1 for 1–7 wt% H₂O. As has been consistently noted by others (e.g. Bartholomew et al., 1980), one observes three bands at (A) 5200 cm⁻¹ $(1.91 \,\mu\text{m})$, (B) $4500 \,\text{cm}^{-1}$ (2.22 μm), and (C) $3900 \,\text{cm}^{-1}$ (2.53 µm); note that these are very weak absorption features that appear at frequencies just above the fundamental OH stretching modes of both X-OH and H₂O, these bands are ~100 times weaker than the fundamental O-H vibrational bands with absorption cross sections near that of the first overtone frequency at $\sim 7100 \, \mathrm{cm}^{-1}$ (not shown). Peaks A-C all increase in intensity with increasing total water content, as has been consistently been observed by many other studies (e.g. Bartholomew et al., 1980, Takata et al., 1981, and Stolper, 1982). Peak A exhibits the greatest response to increased water content, whereas Peak B increases intensity initially and then plateaus at the higher water contents. Peak C is a shoulder on the high frequency

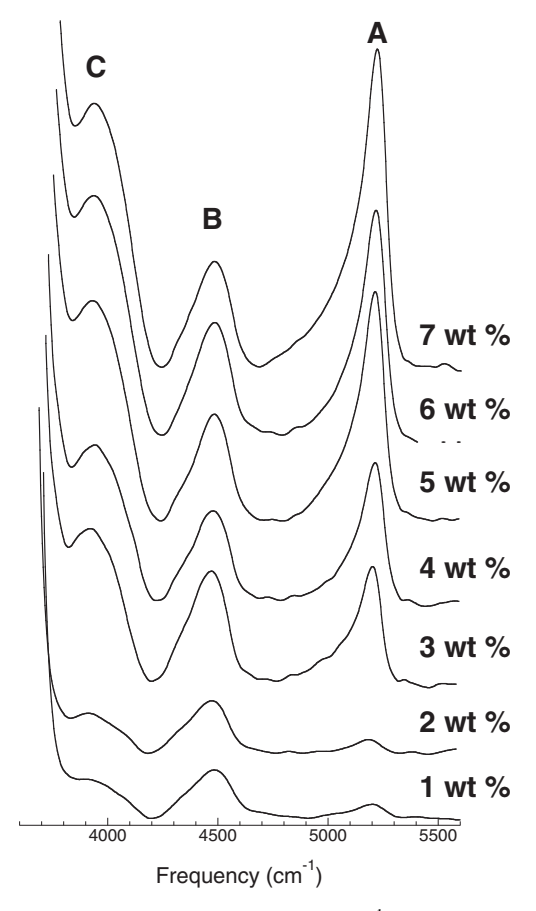


Fig. 1. Near Infrared (NIR) ($3600-5600~{\rm cm}^{-1}$) spectra of hydrous NaAlSi₃O₈ glasses ($1-7~{\rm wt}\%$ total water). NIR band A ($5215~{\rm cm}^{-1}$, 1.91 µm) has been assigned as a combination band that corresponds to H₂O, NIR band B ($4480~{\rm cm}^{-1}$, 2.23 µm) has been assigned as a combination band that corresponds to X-OH, NIR band C ($3940~{\rm cm}^{-1}$, 2.53 µm) is generally assigned as a combination band that corresponds to H₂O and X-OH. The spectra are normalized to sample thickness and offset vertically for clarity.

end of the OH stretching fundamental peak and increases in intensity incrementally with increasing total water content (Fig. 1).

In Fig. 2, the integrated intensities (peak areas) of Peaks A and B, normalized to the thickness of the glass disks, yielding absorbance (signal/sample thickness) (Table 1), are plotted against the nominal water content, the NIR data of Schmidt et al. (2001) are presented as (dashed line) curves for comparison. Notwithstanding the scatter in the present data, one clearly observes that at low water contents, Peak B is dominant over Peak A, but at higher water contents, Peak A continues to grow and becomes predominant. The scatter in the data precludes precise determination as to where the predominance cross-over occurs, but this is likely somewhere between 2.5 and 4 wt%. These data compare well with NIR data (dashed line, Fig. 2) for an identical melt composition (Schmidt et al., 2001) where the predominance cross occurs near 3 wt% total water and also with earlier studies (e.g., Silver and Stolper, 1989). NIR spectroscopy of the felsic glass (FG) was

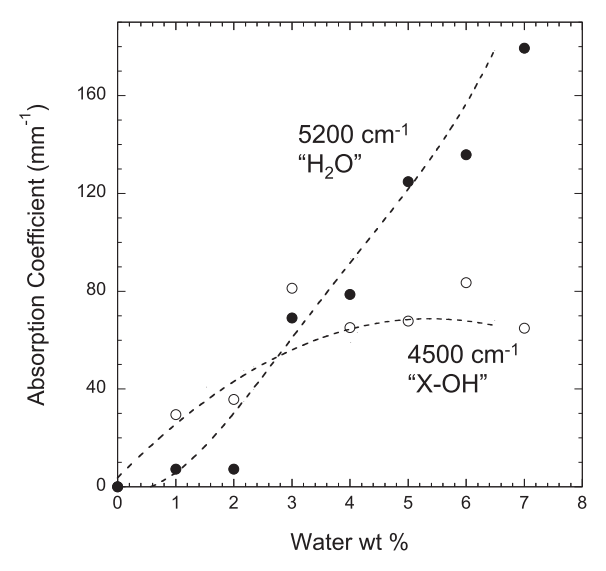


Fig. 2. The absorbance of peaks A (5215 cm⁻¹, black circle) and B (4480 cm⁻¹ open circle), as a function of the total water content. The dashed lines trace the trends for the same bands with water content in a previous study of hydrous NaAlSi₃O₈ glass (Schmidt et al., 2001). These NIR trends are typically interpreted such that at total water contents in excess of 3 wt%, the concentration of H₂O species become predominant over water as X-OH species.

performed only for 1 and 10 wt% and reveals that absorption at \sim 4500 cm⁻¹ ("X-OH") at 1 wt% total H₂O is more intense than absorption at \sim 5200 cm⁻¹ ("H₂O"), but at 10 wt% total water absorption at \sim 5200 cm⁻¹ is much greater than that for the peak at \sim 4500 cm⁻¹ (Table 2).

3.2. ¹H MAS NMR of Hydrous NaAlSi₃O₈ and Rhyolite glasses

A representative expanded ¹H MAS NMR spectrum of hydrous (6 wt% H₂O) NaAlSi₃O₈ glass is presented in Fig. 3 where it is observed that the spectrum is dominated by a broad peak centered at ∼4 ppm and a distinct shoulder at ∼1 ppm. The low frequency shoulder has been observed in ¹H NMR spectra of a range alumino-silicate compositions (Malfait and Xue, 2010), where the intensity of this peak is shown to increase systematically with increased

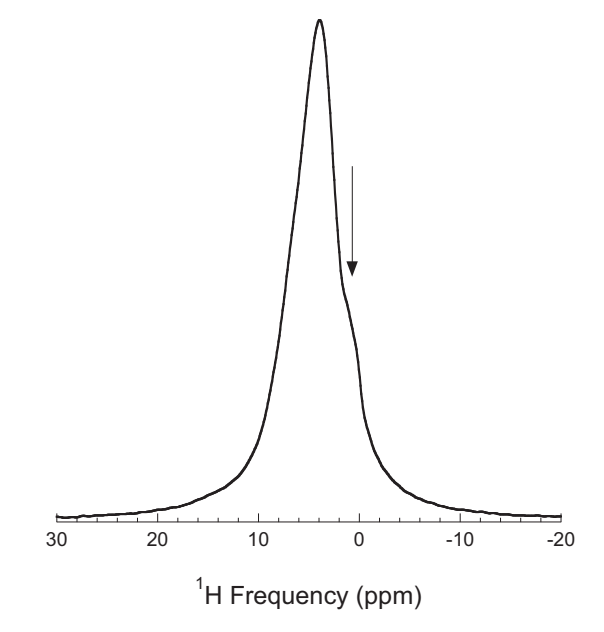


Fig. 3. A representative 1H MAS NMR ($\omega_r/2\pi=22$ kHz) spectrum of a hydrous NaAlSi $_3O_8$ glass (6 wt% H_2O). The spectrum is dominated by a broad peak centered at 4 ppm. There is an obvious shoulder at ~ 1 ppm (arrow) that has been previously shown to be associated with 1H in proximity to aluminum (Malfait and Xue, 2010).

Al/(Al + Si), strongly suggesting that it constitutes some ¹H species associated with aluminum. The full ¹H MAS NMR spectra of variously hydrated NaAlSi₃O₈ glasses (nominal degree of hydration are 1–10 wt%, Table 1) are presented in Fig. 4. For each water concentration, the ¹H MAS NMR spectrum consists of broad peak centered at ~4 ppm. In some case, e.g, at 10 wt% H₂O, there, is also a very sharp peak (~0.2 ppm half width) sitting on top of the low frequency shoulder (Fig. 3) at 0.8 ppm. This sharp peak constitutes a maximum between 1–2 % of the total hydrogen and has been observed in other hydrated silicate glasses (e.g. Eckert et al., 1987, Le Losq et al., 2015b, 2016). Le Losq et al. (2015b) speculated that this minor peak might represent trace amounts of alkali metal OH complexes with no hydrogen bonding. It is, however, the

Table 2
Water content in hydrous Felsic Glass and H NMR determined water speciation.

Nominal water content (wt%)	A4500 ^a	A5200 ^b	ΣSB(1)/CB ^c	Uncertainty	Total water Mol% ^d	X-OH ^e Mol%	H ₂ O Mol%
1.0	1.42	0.66	0.104	± 0.009	3.5	1.4	2.1
3.75	_	_	0.126	± 0.004	12.4	3.4	9.0
5.0	_	_	0.128	± 0.004	16.1	4.3	11.8
7.5	_	_	0.094	± 0.003	22.8	10.5	12.3
10.0	5.25	16.8	0.081	± 0.005	28.8	15.5	13.3

^a Integrated area of 4500 cm⁻¹ peak divided by thickness (mm⁻¹).

b Integrated area of 5200 cm⁻¹ peak divided by thickness (mm⁻¹).

^c Sum of integrated $n \pm 1$ spinning bands divided by the integral of the center band.

d calculated based on formula weight of FG for a single Si,Al tetrahedra.

e X-OH as H₂O.

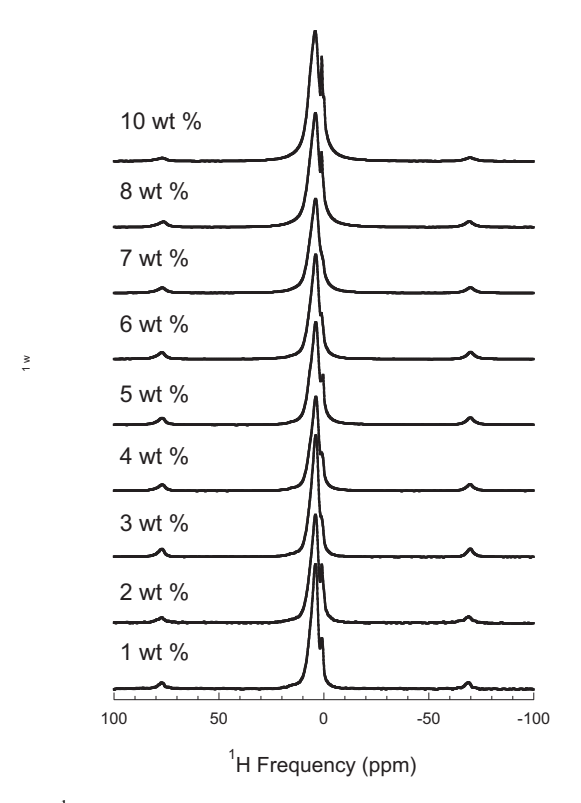


Fig. 4. ^{1}H MAS NMR ($\omega_{r}/2\pi=22~kHz$) spectra of hydrous NaAlSi₃O₈ glasses (1–10 wt% H₂O). The spectra are normalized to total peak area and are offset vertically for clarity. Clearly evident in each spectrum are spinning side bands indicating a degree of dipolar coupling between hydrogen atoms. The sharp peak at low frequency indicates highly mobile H corresponding to 1–2% of the total side band intensity.

identity of this peak is not clear. This peak does not contribute to the side band intensity and the extremely narrow line width indicates highly mobile, liquid like, ¹H species. Note that in all the glasses in this study that both lack and exhibit this sharp peak, there is no optical evidence of fluid inclusions, meaning the glasses were optically clear. In all subsequent discussion and analysis focus is on the main broad peaks (including the shoulder at 1.5 ppm, Fig. 3) and the spinning sidebands. The spectral intensity (1–2%) of these sharp bands are subtracted from the center broad peak that constitutes predominantly H₂O and Si,Al-OH species in all subsequent calculations.

In Fig. 4, for each degree of hydration, the full spectra are presented revealing spinning sidebands at \sim -70 and 76 ppm indicative of a degree of dipolar coupling. What is not obvious in Fig. 4, however, is any progressive increase in side band intensity with water content. Such an increase would signify an increase in the proportion of H_2O over (Si,Al)-OH with increasing water content as would be expected based on the NIR data shown in Figs. 1 and 2 and published by others (e.g. Silver and Stolper, 1989). With increasing H_2O content there is also a noticeable and systematic increase in the width of the center band (Fig. 4); a similar observation was made by Eckert et al. (1988) who concluded that the line broadening was not due to dipolar coupling (i.e. homogenous line broaden

ing) but rather an expansion of the chemical shift range (i.e. inhomogeneous line broadening) with increasing water content.

The ¹H MAS NMR spectra of the variously hydrated FG glasses (nominal hydration 1-10 wt%, Table 2) are presented in Fig. 5. As is the case for the hydrous NaAlSi₃O₈ glasses, sideband intensity is observed for each hydrated FG glass revealing a degree of ¹H-¹H dipolar coupling. There is no obvious increase in side band intensity relative to the center band with increasing water content that would suggest increased proportion of H₂O relative to X-OH as suggested by the NIR data. It is notable that the side band intensity in the hydrous FG samples are systematically slightly more intense than that observed for the hydrous NaAlSi₃O₈ glasses (Figs. 3 and 4 and Tables 1 and 2). What is also evident is that the width of the center band for the hydrous FG glasses is noticeably greater than that for hydrous NaAlSi₃O₈ glasses at any given water content (Figs. 4 and 5).

It is important to recall that the FG glasses contain 0.3 mol % Fe, whereas the hydrous NaAlSi₃O₈ glasses have no Fe. As noted earlier by Eckert et al. (1988), unpaired electrons in Fe will also magnetically (dipole) couple with

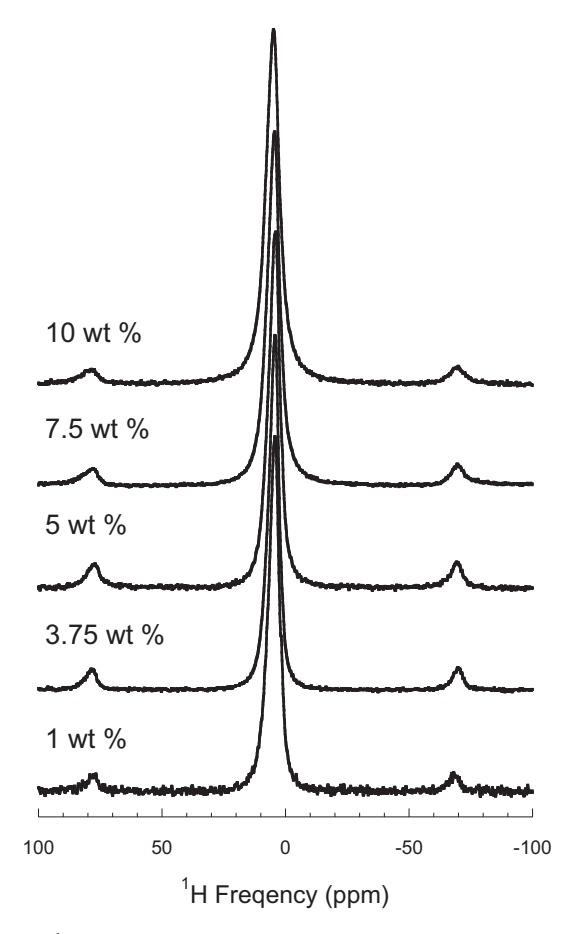


Fig. 5. 1 H MAS NMR ($\omega_{r}/2\pi = 22$ kHz) spectra of hydrous felsic glasses "FG" (1–10 wt% $H_{2}O$). The spectra are normalized to total peak area and are offset vertically for clarity. Clearly evident in each spectrum are spinning side bands indicating a degree of dipolar coupling between hydrogen atoms.

¹H. Therefore, it is likely that some of the side band intensity in the hydrous FG glasses may be due to electron-¹H dipolar coupling. The gyromagnetic moment of an unpaired electron (γ_e) (associated with Fe cations) is \sim 650 times larger than that of 1H. Therefore, even a small amount of Fe can have very strong effect on these ¹H solid state NMR spectra. The center band regions of FG ¹H MAS NMR spectra are slightly wider than what is observed for the hydrous NaAlSi₃O₈ glasses (Figs. 4 and 5), which could also be due to homogenous broadening associated with electron-¹H coupling. Superimposed on this is the observation that the center band line width increases with increased water content (e.g. Eckert et al., 1988), as noted above for the hydrous NaAlSi₃O₈ glasses. This increase in center peak width, however, is again due to inhomogeneous line broadening (i.e. a wider chemical shift range with increased total water content).

3.3. Deuterium (D) NMR results for hydrated $NaAlSi_3O_8$ glasses

In order to assess whether there was a degree of internal consistency with the results of the ¹H NMR experiments, we explored the use of D NMR to determine D speciation (X-OD and D₂O) in hydrous (D₂O) silicate glasses quenched from melt. To the best of our knowledge, Eckert et al., 1987 was the first study to use static deuterium solid state NMR in the context of understanding water speciation in silicate melts. D MAS NMR studies have been subsequently performed on hydrous (D₂O) alkali oxide tetrasilicate glasses (Wang et al., 2015, Le losq et al., 2016).

Our NMR laboratory has only MAS RF probes, therefore, in order to compare the present samples with the earlier static experiments (Eckert et al., 1987), slow MAS was performed to approximate static NMR. Mapping slow MAS to static NMR has been shown to be straight forward (e.g. Herzfeld and Berger, 1980). At MAS frequencies much less than interaction frequencies (e.g. chemical shielding anisotropy, dipolar coupling and quadrupolar coupling) the "static" line shapes are clearly traced across the many closely spaced spinning side bands that very closely emulate that of the static NMR line shape.

MAS D-NMR ($\omega_r/2\pi = 8 \text{ kHz}$) spectra of hydrated (with D₂O at 17.6 mol %) lithium tetrasilicate (LS4), sodium tetrasilicate (NS4), and potassium tetrasilicate (KS4) glasses are presented (Fig. 6). In each D MAS NMR spectrum one observes the shape of the deuterium quadrupolar powder pattern traced out by multiple spinning sidebands (each separated by exactly 8 KHz). The D MAS NMR spectrum of hydrous LS4 glass reports a quadrupolar line shape with a biaxality parameter, η , equal to 1 and a quadrupolar coupling constant, $C_q,\sim 104~KHz$ indicative of D_2O molecules undergoing 180 $^\circ$ flips with a flipping rate on the order of 10⁵ per second (Fig. 6) (Eckert et al., 1987). The D MAS NMR spectrum of hydrous (with D2O) KS4 glass reveals a broadened "Pake" (twin peak) powder pattern (Pake, 1948) (resulting from 2 H's nucleus being quadrupolar with spin I = 1) consistent with predominantly X-OD (Eckert et al., 1987) [note that O-H (and D) bond lengths are much longer than in hydrous

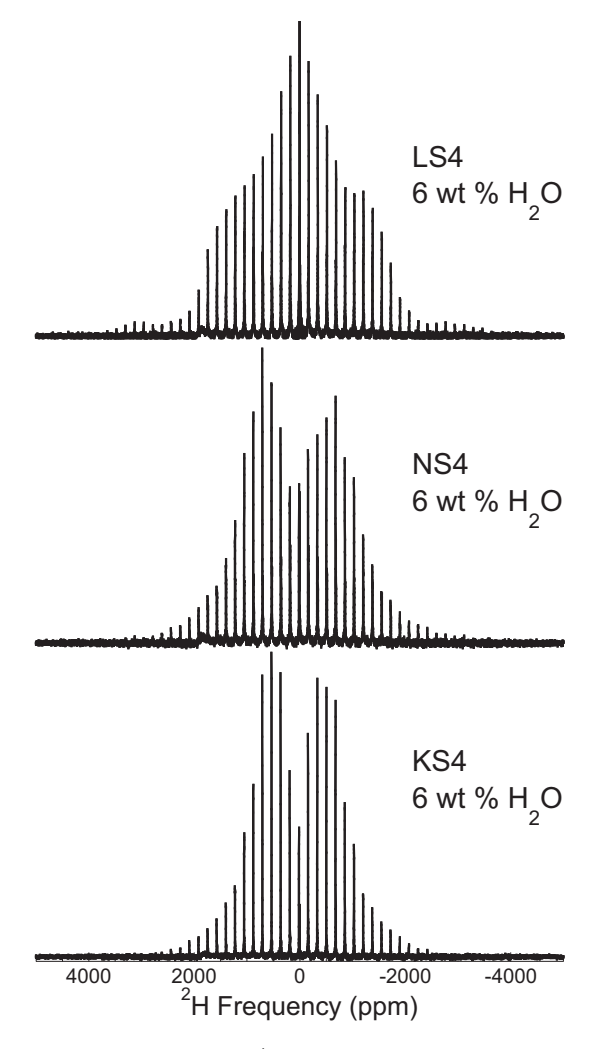


Fig. 6. D MAS NMR ($\omega_r/2\pi=8\,\mathrm{kHz}$) spectra of hydrous (w 17.6 mol % D_2O) lithium, sodium, and potassium tetrasilicate glasses (LS4, NS4, and KS4, respectively). The primary control on the D MAS NMR spectrum is the deuterium quadrupolar coupling constant, C_Q . In each spectrum the multiple spinning side bands trace out the shape of the quadrupolar powder patterns. For hydrous KS4 one observes a broadened classic Pake powder pattern with a symmetery parameter $\eta=0$ and a $C_Q=140\,\mathrm{kHz}$ consistent with rigid X-OD groups. The hydrous LS4 glass exhibits a powder pattern exhibiting no radial symmetry in the electric field gradient around D ($\eta=1$), and a $C_Q=104\,\mathrm{kHz}$ - consistent with D_2O undergoing rapid 180 ° flipping.

NaAlSi $_3O_8$ glasses (Le Losq et al., 2015b), thus the quadrupolar interaction is weaker than that was previously observed for hydrous alumino-silicate glasses (Eckert et al., 1987)], and the KS4 powder pattern records a $C_q \sim 140$ KHz, $\eta = 0$. The D MAS NMR spectrum of NS4 (Fig. 6) records a mixture of LS4 and KS4 line shapes (as has previously been shown in Wang et al., 2015). That water exists as predominantly D_2O species in LS4 and predominantly X-OD species in KS4 is consistent with the earlier 1H MAS NMR study of Le Losq et al (2015b).

In Fig. 7, D MAS NMR spectra (MAS $\omega_r/2\pi = 8$ kHz) are presented for hydrated NaAlSi₃O₈ glasses with D₂O

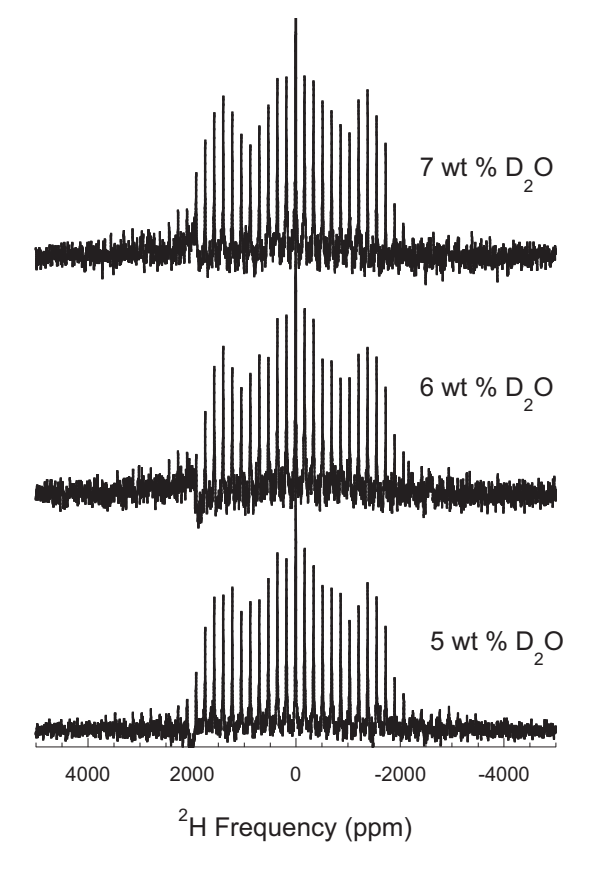


Fig. 7. D MAS NMR ($\omega_r/2\pi=8~kHz$) spectra of hydrous hydrous NaAlSi $_3O_8$ glasses (5, 6, and 7 wt% D_2O). A superposition of two different D powder patterns is observed. The center "peak" arises from a non-radially symmetric electric field gradient powder pattern ($\eta=1$, $C_Q=104~kHz$) associated with D_2O exhibiting rapid 180 ° flipping, the outer peaks correspond to a broadened classic Pake powder pattern (($\eta=0$, $C_Q=204~kHz$) corresponding to rigid X-OD.

contents of 5, 6, and 7 wt% H_2O equivalent D_2O . In each case there is a clear combination of two quadrupolar powder patterns (traced out by the many spinning side bands). The center peak is again interpreted as due to D_2O species undergoing rapid flipping at 180 °C described by $\eta=1$ and $C_q=104$ KHz (Eckert et al., 1987) as is observed for the LS4 glass (Fig. 6). The second quadrupolar powder pattern is a classic Pake pattern ($\eta=0$) due to X-OD species, but the splitting in the two peaks for hydrous NaAlSi $_3O_8$ is significantly larger than that observed for hydrous (D) KS4 (Fig. 6) indicating a $C_q\sim 208$ kHz, that is consistent with O-D distances in hydrous NaAlSi $_3O_8$ being shorter than that in hydrous KS4 (Eckert et al., 1987, Eckert et al., 1988, Xue and Kanzaki, 2004, Le Losq et al., 2015b, 2016, Wang et al., 2015).

3.4. Exploring the effect of water content on glass structure with Silicon (²⁹Si) NMR

In order to determine whether internal consistency exists with the ¹H MAS NMR data we performed ²⁹Si MAS NMR analysis on three FG glasses spanning the full range

of H_2O hydration (0, 5 and 10 wt% H_2O), where the presence of 0.3 mol % Fe enhances the reduction in 29 Si T_1 (spin lattice) relaxation and, thus, vastly increased the S/N over what would have been possible without the presence of Fe (Maekawa et al., 1991). In Fig. 8 29 Si MAS NMR spectra for hydrous FG glasses with 0, 5 and 10 wt% H_2O are presented. The spectra are broad with no obvious shoulders indicative of discrete Q^n species. There is a systematic shift to higher frequency with addition of 5 and 10 wt% H_2O , respectively. A similar progressive frequency shift to higher frequency with increasing total water has been observed in 29 Si MAS NMR of hydrous glasses of NaAlSi₃O₈ and phonolitic composition upon progressive hydration (Olglesby and Stebbins, 2000, Robert et al., 2001).

4. DISCUSSION

4.1. NIR discussion

NIR spectroscopy is commonly used as a method to determine the speciation of water in silicate glasses and melts. The NIR features in consideration are Peaks A (5200 cm^{-1}) and B ($\sim 4500 \text{ cm}^{-1}$) (Fig. 1) that have been interpreted to be combination bands (e.g. Scholtz, 1960). Combination bands are defined as arising in cases where a single photon at a given energy can simultaneously excite two single quantum vibrational transitions where the sum of the vibrational energies equals the energy of the photon (Levine, 1975, Harris and Bertolucci, 1978). These bands arise from anharmonic effects and are typically very weak features relative to the fundamental vibrational modes (Levine, 1975, Harris and Bertolucci, 1978), Peak A (5200 cm⁻¹) is observed in liquid water and opal (SiO₂·nH₂O) (Scholtz, 1960) and has been interpreted to result from the combination of two primary vibrational frequency bands of

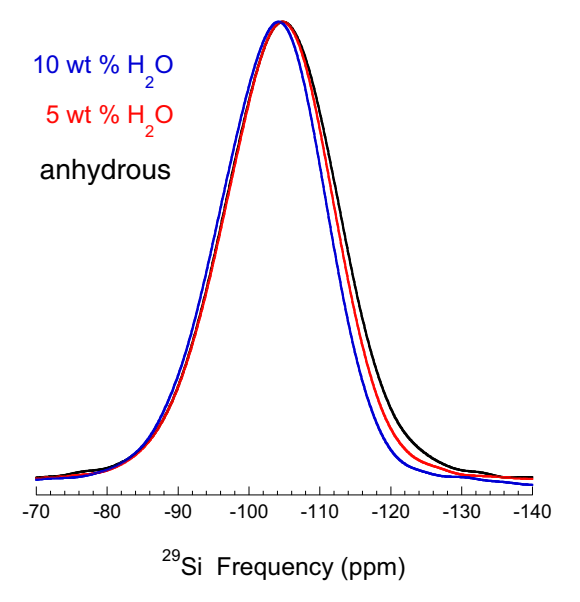


Fig. 8. 29 Si MAS NMR spectra of hydrous FG glass (0, 5, and 10 wt% 49 H₂O) normalized by peak height revealing a progressive shift to higher frequency with increasing water content.

water: the fundamental H_2O stretching at $\sim 3600 \, \mathrm{cm}^{-1}$ (v H_2O) and the H_2O bending mode at $\sim 1630 \, \mathrm{cm}^{-1}$ (δ H_2O). Peak B (4500 cm⁻¹) was observed in muscovite and low water content glasses (Scholtz, 1960, Dodd and Fraser, 1966) and has been interpreted to result from the combination of the fundamental X-OH stretching at $\sim 3600 \, \mathrm{cm}^{-1}$ (vOH) with a Si–OH bending mode at $\sim 920 \, \mathrm{cm}^{-1}$ (δOH) (Scholtz, 1960, Bartholomew et al., 1980) or a Si–O stretching mode at $\sim 920 \, \mathrm{cm}^{-1}$ (vSi–O) (Zarubin, 1999). Zarubin (1999) offered a different interpretation for Peak B ($\sim 4500 \, \mathrm{cm}^{-1}$) where he proposed there might also be a contribution from H_2O via a combination of the fundamental stretching mode and a pair of low frequency librational (ρ) modes.

The interpretation of Peak C (\sim 4000 cm⁻¹) (Fig. 1) is more uncertain. Wu (1980) interpreted Peak C to correspond to a combination band involving Si-OH that was perturbed by strong hydrogen bonding, and concluded that both peaks C and B represented X-OH species. However, in a second paper published from the same laboratory (Bartholomew et al., 1980), no discussion regarding the potential identity or significance of Peak C was provided, rather analysis of (Si,Al)-OH and H₂O compositions was derived considering only Peaks A and B. Takata et al. (1981) accepted Wu's (1980) interpretation for the identity of $\sim 4000 \,\mathrm{cm}^{-1}$ band (Peak C) as they observed evidence of strong H-bonding in the fundamental OH stretching region (vH₂O and vOH) of their hydrous sodium trisilicate glass IR spectra. Stolper (1982), however, noted that in hydrous aluminosilicate glasses there was minimal indication of extensive strong H-bonded OH in the fundamental stretching region and yet a relatively intense peak at ~4000 cm⁻¹ (Peak C) was still clearly evident. Stolper (1982) further showed a linear correlation between the overtone band at $\sim 7000 \text{ cm}^{-1}$ (not shown in Fig. 1) and the 4000 cm⁻¹ (Peak C) band. This led him to conclude that the 4000 cm⁻¹ band likely corresponds to contributions from both H_2O and X-OH (X = Si and/or Al), although no specific assignment was made for this mode. Zarubin (1999) proposed assigning Peak C to exclusively H₂O through a combination of vH2O with a low frequency H_2O librational (ρ) band.

For the purpose of deriving estimates of H₂O and X-OH abundances, all subsequent NIR studies focused exclusively on Peaks A and B. A major benefit of considering only these two peaks is that commonly a linear relationship between measured absorbance and total water content (over a range of water contents) is observed, where from the slope and intercept molar absorption coefficients may be determined (e.g., Zotov and Keppler, 1998, Yamashita et al., 2008). Such linearity would appear to indicate that in many glass systems, variation in water content does not affect change the molar extinction coefficients. This point is particularly interesting because studies of glasses of different compositions (aside from water content) where composition spans a range of NBO/T, large changes in the magnitudes of the extinction coefficients of both the 4500 and 5200 cm⁻¹ bands are reported (Bartholomew et al., 1980, Stolper, 1982, Newman et al., 1986, Silver and Stolper, 1989, Silver et al., 1990, Dixon et al., 1995,

Nowak and Behrens, 1995, Behrens et al., 1996, Yamashita et al., 1997, Withers and Behrens, 1999, Ohlhorst et al., 2001, and Mandeville et al., 2002). In general, extinction coefficients for both bands decrease significantly with increased NBO/T.

Yamashita et al. (2008) showed this same relationship with NBO/T in a study of hydrous sodium silicate glasses with varying Na₂O content, e.g. NS6, NS4, and NS2 $(N = Na_2O, S = SiO_2)$. They suggested that the reduction in extinction coefficients could be due to increased hydrogen bonding going from NS6 to NS2 at a given total water content. However, Cody et al. (2005) also studied hydrous sodium silicate glasses using fast spinning (26 kHz) ¹H MAS NMR from NS8 to NS2 and saw no significant differences in the proportion of hydrogen that exhibit strong H-bonding. Yamashita et al. (2008) also performed static ¹H NMR on their glasses and discovered that the water speciation indicated by ¹H NMR differed significantly from that derived from NIR, they observed much more "OH" than the NIR spectra indicated. Their solution to this discrepancy was to use the ¹H NMR data to calibrate the NIR extinction coefficients by assuming that the magnitude of the extinction coefficients was linearly proportional to the total water content. This calibration maintained a linear relationship between absorbance and total water concentration, but now the slope and intercept of the calibrated data had no simple relationship to the magnitude of the extinction coefficients. This means that ¹H NMR would always have to be used to calibrate NIR in order to derive water speciation for hydrous alkali silicate glasses. However, as shown by Yamashita et al. (2008) a linear dependence of absorbance with total water content does not guarantee that the extinction coefficients for the 4500 and 5200 cm⁻¹ peaks are invariant with variation in total water content. This result is significant as it suggests that, in general for hydrous glasses of any composition, ¹H NMR spectra should always be obtained to ensure calibration and consistency of the NIR extinction coefficients. It should also be noted that much earlier Zhang et al. (1997) concluded that there must be a dependence of water concentration on the molar absorptivity of the 4500 cm⁻¹ band in hydrous rhyolitic glasses.

A systematic study of the potential effect of hydrogen bonding on NIR spectroscopy of hydrous glasses involved focusing on lithium, sodium, and potassium tetrasilicate glasses (LS4, NS4, and KS4, respectively) with variation in total water content (Le Losq et al., 2015a). ¹H MAS NMR clearly revealed that the nature of the alkali cation in simple hydrous alkali tetrasilicate glasses has a very strong effect on the proportion of water derived hydrogen exhibiting long O-H bonds, plausibly due to H-bonding interactions (Le Losq et al., 2015b). This proportion ranges from $\sim 27\%$ for LS4 up to $\sim 89\%$ for KS4 (Le Losg et al., 2015b). Le Losq et al. (2015a) showed that changes in alkali metal has a very strong effect on the mid-IR spectra of hydrous alkali silicate glasses, for example, the intensity of the fundamental stretching band at 3500 cm⁻¹ decreases by ~10 times moving from LS4 to KS4; this is a much bigger drop than suggested by the NMR determination of differences in proportions of H in strong H-bonding interactions.

Le Losq et al. (2015a) also studied the NIR region and showed that the intensity of the 5200 cm⁻¹ band dropped by ~18 times moving from LS4 to KS4. As the 5200 cm⁻¹ is interpreted to be a combination band involving the fundamental at 3600 cm⁻¹, such a drop in intensity would be expected (Zarubin, 1999). Interestingly, the NIR data of Le Losq et al. (2015a) did not also show a similar reduction in the intensity of the 4500 cm⁻¹ band moving from LS4 to KS4. Although the NBO/T of the dry alkali tetrasilicate glasses are the same, this is not the case for the hydrous glasses. Rather the NBO/T for hydrous KS4 is much larger than that of LS4 (Le Losq et al., 2015b). The drop in intensity of the 5200 cm⁻¹ band intensity from LS4 to KS4 could be the result to the loss of intensity at 3500 cm⁻¹ due to increased H-bonding (Zarubin, 1999), a simultaneous reduction in H₂O speciation based on composition and/or reduction of the extinction coefficient with increasing NBO/T as shown by Yamashita et al. (2008). It is not possible to sort out which effect contributes more or less. This means for studies where the proportion of H-bonded H's changes significantly, NIR cannot provide robust estimates of speciation (Le Losq et al., 2015a). Again, ¹H NMR is required to assess water speciation.

4.2. ¹H-¹H dipolar coupling in static and MAS ¹H NMR

For hydrogen in silicate glasses, the primary control on the ¹H chemical shift is oxygen-hydrogen bond distance (e.g. Eckert et al., 1988; Xue and Kanzaki, 2004). Unfortunately, the chemical shift cannot uniquely distinguish X-OH and H₂O. As noted earlier, Malfait and Xue (2010) did identify a low frequency peak/shoulder in the ¹H NMR spectra of hydrous alumino silicate glasses that they attributed to ¹H spatially close to ²⁷Al. Malfait and Xue (2010) inferred that this ¹H NMR feature was likely Al-OH based on NIR data and low total water content, but beyond noting close ²⁷Al proximity it is not possible to definitively rule out this feature arising from molecular H₂O being close to ²⁷Al.

In addition to chemical shielding there is another significant interaction that profoundly affects the solid-state ¹H NMR spectra. Homonuclear dipolar coupling arises from the magnetic interaction of one or more ¹H on a neighboring ¹H. In ¹H bearing solids, strong dipolar coupling between protons can be the dominant interaction affecting the ¹H NMR spectrum. For example, at moderate static magnetic field strength (e.g. 7 Tesla in the present case) ¹H chemical shielding anisotropy can be as large as 9 kHz (Mehring, 1976), while the strength of dipolar coupling of two hydrogens in rigid water molecules, e.g. gypsum, is on the order of 33 kHz.

The strength of dipolar coupling is governed by the magnitude of the dipolar coupling constant (B_{12} , Eq. (2)) that is determined both by the magnitude of the magnetic moments of the nuclei, given by the gyromagnetic ratio ($\gamma_{1,2}$), as well as the internuclear distance (r_{12}) (note, overall dipolar coupling interactions are also governed by the orientation of the internuclear vector with respect to the main magnetic field. In a powder the orientation of the internuclear vector is random and with static 1H NMR this leads

to the observation of the classic twin peaked "Pake" powder pattern (Pake, 1948). In Eq. (2) the magnetic constant, μ_0 , and Planck's constant, \hbar , are also included;

$$B_{12} = \frac{\mu_0 \gamma_1 \gamma_2 \hbar}{4\pi (r_{12})^3} \tag{2}$$

As the magnitude of the dipolar coupling constant, B_{12} , scales as the inverse cube of the internuclear distance, the magnitude of dipolar coupling decays very quickly as r₁₂ increases. In Fig. 9 the magnitude of the dipolar coupling constant, B₁₂, for a pair of protons, is plotted against ¹H-¹H distance. For example, for a ¹H-¹H distance of 1.5 Å, ca. the distance between two hydrogens in H₂O, $B_{12} \sim 36$ kHz. Historically, static ¹H NMR provided the first estimate of ¹H-¹H distance for water molecules in gypsum (Pake, 1948), where Pake used his static NMR data to fit the "Pake" pattern to estimate the magnitude of B₁₂ leading to an estimated value for r_{12} being 1.58 Å. As protons are essentially invisible to X-rays, this estimate remained for a long time as the definitive measure of ¹H⁻¹H distance of H₂O in gypsum; more recently refinement of neutron diffraction data for gypsum indicates that H-H distance (r₁₂) is actually 1.53 Å (Pedersen and Semensen, 1982), where based on Eq. (2) one finds that B_{12} would be 33.3 kHz.

All of the 1H solid-state NMR experiments performed in this study employ magic angle sample spinning (MAS) at a frequency ($\omega_r/2\pi$) of 22 kHz. Whereas fast MAS will average out some of the effects of dipolar coupling for coupled 1H 's at short distances, 22 KHz is insufficient to completely average out such strong dipolar interactions. The residual dipolar coupling is manifested with MAS as spinning sidebands that reside at exactly at \pm n times the MAS frequency (n = 1,2, ...). In Fig. 10a a 1H MAS NMR

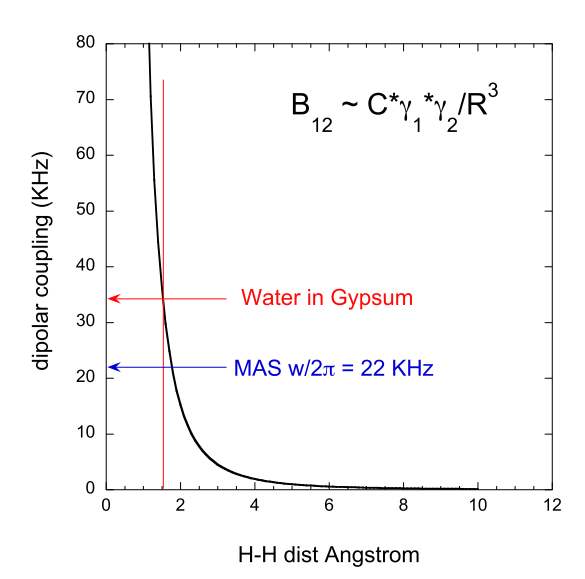


Fig. 9. The magnitude of the dipolar coupling constant (B_{12} , in kHz) as a function of 1H - 1H distance (in angstroms). Water in gypsum ($CaSO_4$ - $2H_2O$) has a 1H - 1H distance of 1.53 Å and $B_{12}=33.3$ KHz. This substantially exceeds the magic angle spinning frequency ($\omega_r/2\pi=22$ KHz) and 1H MAS NMR of gypsum will exhibit strong spinning side bands.

spectrum of gypsum (CaSO₄·2H₂O) is compared with a ¹H MAS NMR spectrum of dry (solid) silicic acid. In gypsum all hydrogen is in the form of H₂O, so in addition to the center band at a chemical shift of ~4 ppm there are also relatively intense side bands at ca. ~76 and ~70 ppm (± 22 kHz off the center band, Fig. 10a); these peaks are present because the MAS frequency ($\omega_r/2\pi = 22$ kHz) is insufficient to average completely the relatively strong dipolar interaction between ¹H in water (B₁₂ = 33.3 kHz) to zero (Fig. 9).

In the case of dry silicic acid all of the water exists as Si-OH's where the actual number of OH's per silicon tetrahedron can only be determined through ²⁹Si MAS NMR (Fig. 10b). It is seen in Fig. 10b that the degree of silica polymerization ($Q^{n=4-0}$, n = number of bridging oxygens to other tetrahedra) is actually quite high with 60 % Q⁴ (no OH), 32 % Q^3 (Si-OH), and 8 % Q^2 (Si-(OH)₂); this means that 33 % of ¹H in this silicic acid sample is in Q² and 67% ¹H is in Q³. In the case of Q² species the two hydrogens per tetrahedron are in somewhat close proximity, e.g. the distance between two ¹H in Q² is estimated to be $\sim 2.5 \text{ Å}$ with a dipolar coupling constant, B_{12} , on the order of 8 kHz (Fig. 9). The internuclear distance of hydrogen in O³ with potentially neighboring hydrogens will vary considerably depending in the identity of the next nearest neighbors, i.e. either Q⁴, Q³, or Q². As the total concentration of water is \sim 10 mol % in the silicic acid, it is likely that Q^3 Si-OH groups are separated sufficiently from other Q^2 and other Q³ species such that minimal dipolar coupling would be expected. The ¹H MAS NMR spectrum of silicic acid (Fig. 10a) verifies this as it exhibits essentially no spinning side band intensity. Eckert et al., 1988 chose tremolite [Ca₂Mg₅Si₈O₂₂(OH)₂] as their "X-OH" standard, where the shortest inter-nuclear proton distance (r_{12}) is $\sim 4.5 \text{ Å}$ and

their ¹H MAS NMR spectrum (at a much lower MAS frequency = 8 kHz) confirms this a good choice as it reveals only weak spinning side band intensity at 8 kHz MAS and would yield virtually no apparent spinning side band intensity at 22 kHz MAS.

4.3. Determining X-OH and H_2O speciation with 1H MAS NMR

In order to determine the speciation of water in hydrous glasses, the integrated intensity of the n = 1 and -1 spinning sidebands (ΣSB) are divided by the integrated intensity of the central spectrum (CB). $\Sigma SB(1)/CB$ ratios for both the hydrous NaAlSi₃O₈ and FG samples were determined and listed in Tables 1 and 2. This parameter is expected to vary from what is expected for 100 % H₂O, e.g. gypsum (CaSO₄·H₂O) or analcite (NaAlSi₂O₆·H₂O), and 100 % X-OH, e.g. silicic acid or tremolite respectively, e.g. Eckert et al. (1988). Based on our ¹H MAS NMR analysis of gypsum, and confirmed by numerical NMR simulations of rigid H₂O assuming a ¹H-¹H distance of 1.53 Å, we conclude that with purely rigid H_2O in a solid and $\omega_r/2$ - $\pi = 22 \text{ kHz}$ one will observe a $\Sigma SB(1)/CB$ ratio of 0.34 (Fig. 11). However, measurement of analcite under the same conditions reveals a $\Sigma SB(1)/CB$ ratio of 0.21, this reduction in $\Sigma SB(1)/CB$ suggests that while water is highly rigid in gypsum, water molecules are slightly more mobile in analcite. A small degree of random H2O motion will reduce B_{12} (Eq. (2)).

Either of these " H_2O " standards (gypsum or analcite) are reasonable based on mineral structure, but the assumption that H_2O in either mineral has similar rigidity (no random motion) in their respective crystal structures is not supported by published data. More significantly, such rigid-

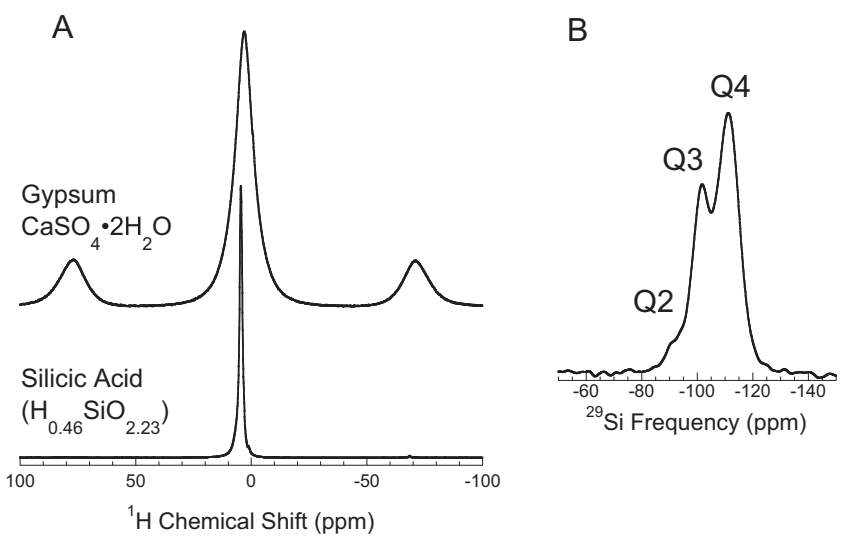


Fig. 10. (A) 1H MAS NMR ($\omega_r/2\pi=22~kHz$) spectra of gypsum (CaSO₄·2H₂O) (top) and solid silicic acid (H_{0.46}SiO_{2.23}). Substantial dipolar coupling of hydrogen atoms is indicated by strong spinning side bands at frequencies \pm 22 kHz on either side of the center band, these are indicated for gypsum (100 % H₂O), but not for silicic acid (100 % X-OH). (B) a 29 Si MAS NMR spectrum of solid silicic acid revealing the concentrations of Q⁴ (no OH), Q³ (1 OH), and Q² (2OH) species. 1 H- 1 H distances in Q² (2OH) species are estimated to be \sim 2.5 Å and experience weak dipolar coupling. Assuming that Q³ (1 OH) will have predominantly Q⁴ (no OH) neighbors, silicic acid is expected to have very weak (undetectable) spinning sidebands.

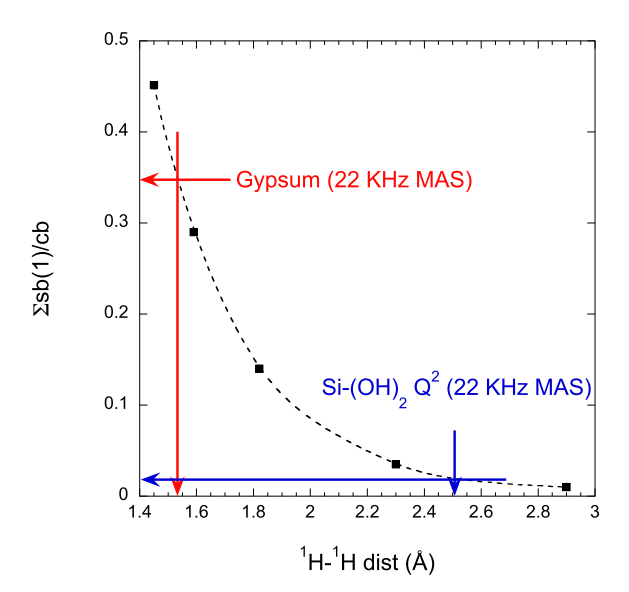


Fig. 11. Simulation of the ratio of the side band (\pm 22 kHz) intensity to the center band intensity ($\Sigma SB(1)/CB$) as a function of 1H - 1H distance for 1H MAS NMR spectra with a MAS frequency ($\omega_r/2\pi$) = 22 kHz), for gypsum (100 % H₂O) with a 1H - 1H distance of 1.53 Å, $\Sigma SB(1)/CB$ is 0.34, which is what is measured in the actual 1H MAS NMR spectrum of gypsum.

ity of H₂O molecules is not actually observed in aluminosilicate glasses (Eckert et al., 1988, Zavelisky et al., 1999, Riemer et al., 2001, Schmidt et al., 2001), instead H₂O molecules move slightly (to some degree and randomly) in hydrous alumino-silicate glasses and such random positional fluctuations reduce (but do not negate) the magnitude of dipolar coupling. This internal motion works in addition to what MAS does in reducing intensity of the spinning side bands. The partial mobility of H₂O species in hydrous alumino-silicate glasses needs to be accounted for when using ¹H MAS NMR to assess X-OH and H₂O concentrations.

Previous studies of static ¹H NMR of hydrous NaAlSi₃-O₈ and alumino-silicate glasses using variable temperature enable an assessment of the mobility reduction on dipolar coupling (Bartholomew and Schreurs, 1980, Eckert et al., 1988, Zavelsky et al., 1999, Riemer et al., 2001, Schmidt et al., 2001). From these studies it is revealed that the rigidity of H₂O in hydrous glasses is temperature dependent (Bartholomew and Schreurs, 1980, Zavelsky et al., 1999, Riemer et al., 2001, and Schmidt et al., 2001), where dipolar coupling strength increases as temperature is reduced. Interestingly, the magnitude of dipolar coupling at the lowest temperature studied, T = 140 K (Riemer et al., 2001), is still much less than what is detected in gypsum (apparently completely rigid with regards to ¹H NMR), i.e., B₁₂ for H_2O in alumino-silicate glass at 140 K is \sim 28 kHz. If the magnitude of B₁₂ of H₂O species in hydrous NaAlSi₃O₈ glass at 140 K reflects rigid H₂O molecules, then a value of B₁₂ of 28 KHz would indicate a ¹H-¹H distance for H_2O to be 1.63 Å (Eq. (2)). However, if this were the case, then one would observe a significant shift in ¹H NMR frequency to much higher frequencies relative to what is observed for H₂O in hydrous NaAlSi₃O₈ glasses (Eckert

et al., 1988, Xue and Kanzaki, 2004). More likely, even 140 K is not cold enough to completely cease $\rm H_2O$ motion in these glasses. Extrapolating the variable temperature data of Riemer et al. (2001) down to a temperature where $\rm B_{12}$ would be equal to what is observed for gypsum (i.e., $\rm B_{12} = 33.3~kHz$) reveals that a temperature of $\sim 90-100~k$ would be predicted to be sufficient to achieve total $\rm H_2O$ immobility.

It is clear that in order to exploit dipolar coupling via ¹H MAS NMR to extract X-OH and H₂O speciation at room temperature the data need to be constrained by the measured dipolar coupling associated with H₂O in these specific (e.g. NaAlSi₃O₈) glasses at room temperature. A number of studies (Eckert et al., 1988, Zavelisky et al., 1999, Riemer et al., 2001, and Schmidt et al., 2001) have shown via static ¹H NMR that the strength of dipolar coupling at room temperature for hydrous NaAlSi₃O₈ glasses is consistently around 22.8 KHz, this is nearly 2/3 that measured for H_2O in gypsum. Thus, a value of $B_{12} = 22.8$ KHz is used to constrain the pure H₂O end member in the present study in order to determine X-OH and H₂O concentrations in hydrous NaAlSi₃O₈ and FG glasses from the magnitude of $\Sigma SB(1)/CB$. A numerical simulation performed under identical MAS conditions ($\omega_r/2\pi = 22 \text{ kHz}$) indicates for $B_{12} = 22.8$ KHz the magnitude of $\Sigma SB(1)/CB = 0.175$ for 100 % molecular H₂O in an alumino-silicate glass at room temperature.

The apparent speciation of H₂O and X-OH (in water equivalents) in hydrous NaAlSi₃O₈ and FG glasses derived from these ¹H MAS NMR data are presented in Fig. 12 a and b. With increasing total water content, initially H₂O species are predominant over X-OH, but at higher total water content, X-OH becomes predominant. These species abundances, as a function of total water content, are completely different from that predicted by the NIR spectroscopy here (Figs. 1 and 2) and repeatedly reported by others for hydrous NaAlSi₃O₈ glasses (e.g. Silver and Stolper, 1989, Schmidt et al., 2001). The same is true for the hydrous FG glasses (Fig. 12b). In general, the proportion of H₂O species at any given water content for the FG glasses is predicted to be greater than for the hydrous NaAlSi₃O₈ glass and the predominance cross over occurs at higher total water content. Recalling that the FG glasses contain 0.3 mol % Fe and noting that dipolar coupling between Fe(e⁻) and ¹H could increase the intensity of the spinning side band intensity beyond that for ¹H–¹H alone (e.g. Eckert et al., 1988), it is certainly possible that the apparent increase in the concentration of H₂O species in the FG glasses (relative to the hydrous NaAlSi₃O₈ glasses) for a given total water content is derived from Fe(e⁻)-H dipolar interactions.

4.4. Water speciation X-OD and D2O from Deuterium NMR

D-NMR also has the potential to reveal X-OD and D_2O speciation (Eckert et al., 1987). As a matter of introduction to D NMR of hydrous silicate glasses, it is noted that mass effects on the equilibrium between "water" and "silanol" (equation (1)) are expected to be minimal with respect to what differences NMR or NIR can show us. A second issue

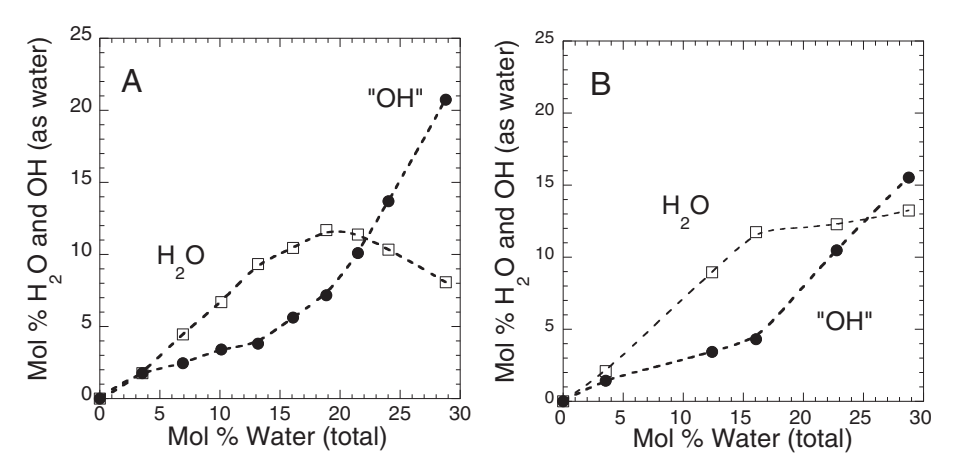


Fig. 12. The speciation of H_2O and X-OH (in mol %, as water) derived from ¹H MAS NMR ($\omega_r/2\pi = 22 \text{ kHz}$) spectra using measured sideband to center band ratios ($\Sigma SB(1)/CB$) for A) hydrous NaAlSi₃O₈ glasses and B) hydrous FG glasses.

is that the ${}^{1}H$ nucleus is a spin I = ${}^{1}/_{2}$ system, whereas the deuteron is a spin I = 1 system, where the quadrupolar interaction plays a significant role in D NMR behavior. The magnitude of the deuteron gyromagnetic ratio (eq. (2)) is 6.5 times smaller than that of ¹H. Therefore, ²H-²H dipolar coupling is much weaker than 1H-1H dipolar coupling (B₁₂ for deuterons in D₂O, assuming ²H-²H distance equal to 1.53 Å, is \sim 42 times weaker than for $^{1}H_{-}^{1}H$ in H₂O, Eq. (2)). For deuterons, the most significant interaction is the quadrupolar interaction, where a key parameter is the quadrupolar coupling coefficient, Co, that for deuterons bonded to oxygen in silicate melts is on the order of ~ 100 to 250 kHz (Eckert et al., 1987). The D(²H) quadrupolar interaction is considerably stronger than the dipolar interaction between protons (¹H) and very much more so for dipolar coupling between deuterons (²H).

A single deuteron, being a spin I=1 system, intrinsically has two energy transitions with differences in frequency derived through the quadrupolar interaction (Slichter, 1996, Levitt, 2009). In this regard, D-NMR of a single rigid deuteron exhibits similar spectral behavior to that of a pair of 1H 's that are strongly dipolar coupled (Slichter, 1996, Levitt, 2009), i.e., both a single $D(^2H)$ and a close pair of 1H 's will exhibit similarly shaped Pake powder patterns in static solid state NMR (where the Pake splitting for a pair of 1H coupled spins is equal to $^3/2$ B_{12} , but where the splitting for an isolated D is equal to $^3/4$ C_O) (Levitt, 2009).

As shown in Fig. 6 rapid 180° flipping of D_2O molecules (on a correlation time scale near the magnitude of quadrupolar coupling, $t_c \sim 10^{-5}$ seconds, Eckert et al., 1987) can profoundly affect the D-NMR powder pattern, transforming the spectrum from a classic "Pake" power pattern (with its characteristic two peaks) into a symmetric single peak powder pattern (e.g. Fig. 6). This is due to the fact that the rapid flipping motion of D_2O changes the nearly purely radial symmetry of the electric field gradient (defined by the biaxality parameter η , where for pure radial symmetry $\eta = 0$) for D bonded to O into a time averaged symmetry that lacks any radial symmetry ($\eta = 1.0$) Eckert et al. (1987). As noted by Eckert et al. (1987) an X-OD is not expected to be subjected to such a "flipping" mode;

thus for static D-NMR, the presence of "X-OD" will be manifested by a classic Pake powder pattern (e.g., $\eta=0$, $C_q=204$ KHz), where D_2O species will be observed by a single broad peak ($\eta=1$, $C_q=104$ KHz), observed between the Pake features of X-OD, e.g. Fig. 6 and Eckert et al. (1987).

Of course, in the case of static ¹H NMR, it is H₂O molecules that will create the Pake powder pattern, while X-OH will contribute a single peak lying between the Pake peaks. This then leads to a potentially confusing observation. As OH (OD) and H₂O (D₂O) species vary with changes in total water content, the ¹H static NMR and D (²H) static NMR spectra, while similar in appearance, will trend in opposite directions with apparent variation in center band vs Pake powder pattern intensity as species change with total water content (e.g. Eckert et al., 1987, Eckert et al., 1988, Zavelisky et al., 1999, Schmidt et al., 2001).

4.5. D MAS NMR of deuterated NaAlSi₃O₈ glasses

Eckert et al. (1987) proposed that the powder patterns of deuterated alumino-silicate glasses, as seen in Fig. 6, indicate a mixture of D₂O and X-OD species. From the earlier ΣSB(1)/CB analysis for our hydrous NaAlSi₃O₈ glasses, we have an estimate of the concentrations of "H2O" and "X-OH" (Fig. 12 and Table 1). It is then interesting to see whether the D MAS NMR data are consistent with the ¹H MAS NMR data (Fig. 12, Table 1). In Fig. 13a D NMR (static) spectra are simulated assuming a composite of two powder patterns (D₂O: $C_q = 104$ KHz $\eta = 1$, and X-OD: $C_q = 208$ KHz $\eta = 0$) and using the ¹H MAS NMR estimates of H₂O and X-OH as a function of water content (Fig. 12, Table 1). As shown in the H MAS NMR data (Fig. 12) as water content increase from 5 to 7 wt%, the peaks associated with the Pake powder pattern (X-OD) should increase relative to that of D₂O. The simulated powder patterns are very similar to the observed D MAS NMR spectra (Fig. 7) and with speciation predicted from the ¹H MAS NMR experiments (Fig. 12).

This simulation can be contrasted with one where the " H_2O " and "X-OH" speciation was determined by static

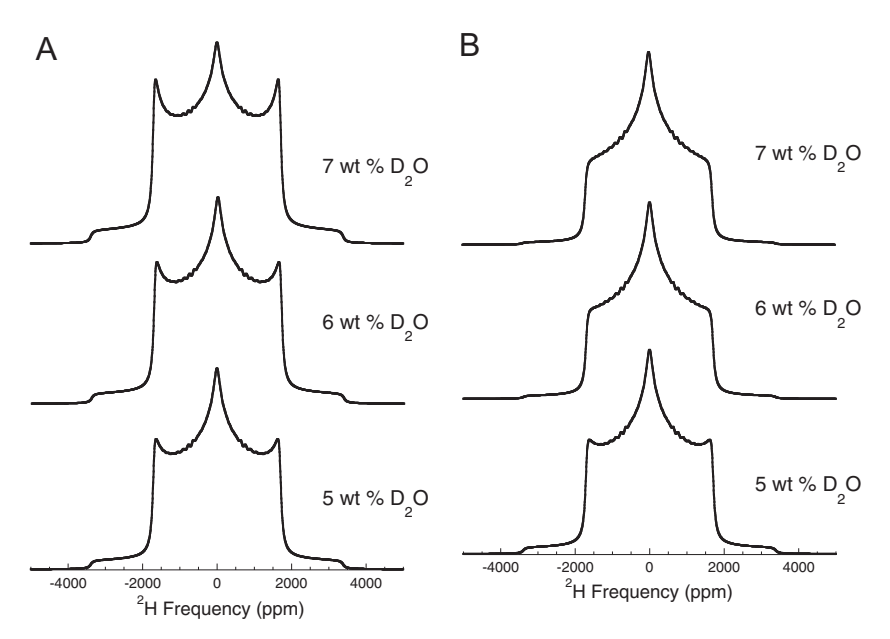


Fig. 13. (A) A simulation of static D NMR spectra using H_2O and X-OH speciation derived from 1H MAS NMR ($\omega_r/2\pi = 22 \text{ kHz}$) (this study), for total water (D_2O) contents of 5, 6, and 7 wt%. (B) A simulation of static D NMR spectra using H_2O and X-OH speciation derived from previous static 1H NMR data (Schmidt et al., 2001), for total water (D_2O) contents of 5, 6, and 7 wt%.

¹H NMR (Schmidt et al., 2001) for hydrous NaAlSi₃O₈ glass at the same total water concentration (which is what is also suggested by the NIR data presented in Figs. 1 and 2 and previously by others). These simulations are presented in Fig. 13b. It is clear that the simulated spectra in Fig. 13b do not recreate what is observed in the D MAS NMR for D₂O containing NaAlSi₃O₈ glasses (Fig. 6). Therefore, the present D MAS NMR spectra report water speciation that are consistent with those derived from the present ¹H MAS NMR data (Fig. 12 and Table 1).

4.6. ²⁹Si NMR Discussion

²⁹Si MAS NMR spectroscopy is particularly instructive for studying the effect of water in the case of hydrous peralkaline glasses (e.g., XS_y , where $X = Li_2O$, Na_2O , and K_2O , $S = SiO_2$ and y = number of SiO_2 per X) because the individual bonding environments for silicon (the socalled Qn species) are clearly resolved in frequency (Maekawa et al., 1991, Kummerlen et al., 1992, Zotov and Keppler 1998, Robert et al., 2001, Xue and Kanzaki, 2004, Cody et al., 2005, Wang et al., 2015, Le Losq et al., 2015b). In the case of hydrous alkali silicate glasses changes in Oⁿ species with addition of water (e.g. Eq. (1)) can be unambiguously observed and quantified. Recently, Le Losq et al. (2015b) compared hydrous (17.6 mol % H₂O) with anhydrous LS4, NS4, and KS4 glasses and used ²⁹Si MAS NMR to show that whereas water depolymerizes LS4 glass only slightly (H₂O dominant), almost all of the water added to the KS4 glass results in depolymerization (X-OH dominant). The predominance X-OH in KS4 hydrous glasses is also indicated by the D NMR spectra in Fig. 6.

Unfortunately, with alumino-silicate glasses (e.g. Zavelisky et al., 1999, Olglesby and Stebbins, 2000, Robert et al., 2001, and here) distinct Qⁿ species resolution is not possible because extensive line broadening creates too much peak overlap for clear species resolution in the ²⁹Si NMR spectra. The principal causes of peak broadening in ²⁹Si MAS NMR spectra of alumino-silicate glasses arise from variation in Si-O-Si and Si-O-Al bond angles (Smith and Blackwell, 1983, Mauri et al., 2000), variation in the Al/Si abundance (Lippma et al., 1980, 1981), variation in the degree of aluminum avoidance (Lee and Stebbins, 1999) and in the case of hydrated glasses, the number and distribution of Si-(OH)_{n=1-4} Q³-Q⁰ species (e.g. Maekawa et al., 1991, Kummerlen et al., 1992, Zotov and Keppler, 1998, Cody et al., 2005).

It is not possible to deconvolve reliably the nearly featureless ^{29}Si NMR spectra of alumino-silicate glasses (e.g. Fig. 8). In order to highlight the changes in the spectra that occur upon addition of total water of 5 and 10 %, we employ difference spectroscopy, where normalized spectra (to equivalent area) are subtracted from each other, i.e., $5\,\text{wt}\%-0\,\text{wt}\%$ and $10\,\text{wt}\%-0\,\text{wt}\%$, respectively (Fig. 14). What is observed is that from 0 to $5\,\text{wt}\%$ H₂O, there is a loss in intensity at $\sim\!-115\,\text{ppm}$ (Q⁴) and a gain intensity at $\sim\!-105$ (Q³) ppm and a shoulder at $-90\,\text{ppm}$ (Q²). The magnitude of the difference peaks, losses and gains, are even greater in the 10–0 wt% difference spectrum. The shifts in spectral intensity (Fig. 7) and the magnitudes of the difference spectra (Fig. 14) clearly increase from $5-0\,\text{wt}\%$ to $10-0\,\text{wt}\%$.

These changes are consistent with continued depolymerization of the FG glass up to the highest water content. It should be noted, however, that this conclusion assumes a high degree of aluminum avoidance (Al-O-Al) that is

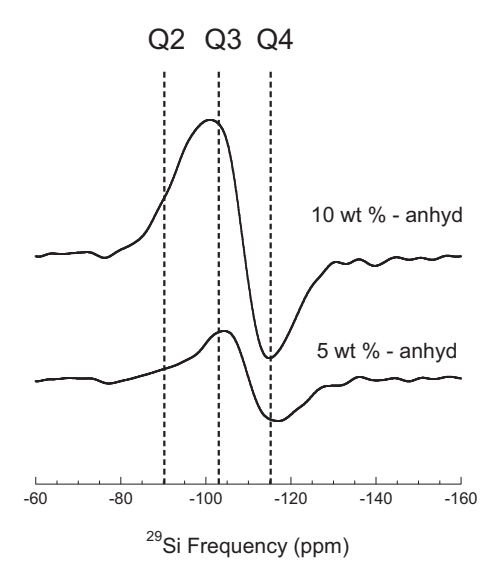


Fig. 14. 29 Si MAS NMR difference spectra (normalized to integral), 5 wt% - anhydrous (bottom) and 10 wt% - anhydrous (top). The dashed lines approximate frequencies of silicon Q^n species, Q^4 (right), Q^3 (middle), and Q^2 (left). The growth of intensity at the higher frequencies is consistent with continuous depolymerization of silicate glass with increasing water content up to 10 wt% water.

expected for NaAlSi₃O₈ glasses (Lee and Stebbins, 1999). If, for some unknown reason, increasing water content decreases aluminum avoidance, then a slight high frequency shift as is observed in Figs. 8 and 14 could occur. We are unaware, however, of any reason why increased water content would decrease aluminum avoidance.

The ²⁹Si MAS NMR data are, therefore, qualitatively consistent with the ¹H MAS NMR and limited D NMR data, even as NIR data (Fig. 2) suggest that depolymerization (indicated by the 4500 cm⁻¹ band) plateaus after ~3 wt. %. Due to the total lack of constraint on species line shapes it is not possible to quantify the degree of depolymerization (as was possible with hydrous alkali tetrasilicate glasses, Le Losq et al., 2015b) only gross chemical trends can be inferred.

4.7. Discrepancy between ¹H NMR and NIR results

The present ¹H MAS NMR analysis (Fig. 12) yields water speciation that is inconsistent with the NIR band analysis (Fig. 2). Focusing on the ¹H MAS NMR analysis, the physics of dipolar coupling is straightforward and well established. If we assume that the NIR assessment is correct then we must consider whether there is something about the ¹H MAS NMR experiments that leads to a false representation of the apparent dipolar coupling interactions that would lead to a distorted assessment of X-OH and H₂O speciation. Solid State NMR spectroscopy is a time resolved emission based spectroscopy and is, potentially, subject to an array of dynamical aspects that could distort spectra if care is not taken with the choice of experimental parameters. Experimental factors that potentially could lead to erroneous estimates for X-OH and H₂O species con-

centration include external (instrumental) factors such as RF pulse power-pulse width, digitizer limits, and pulse recovery time (acquisition delay, AD) and internal factors such as molecular mobility, dense clustering of ¹H-species and differential longitudinal relaxation (1/T₁) rates amongst ¹H species. Any of these have the potential to affect the NMR signal and could potentially lead to erroneous determination of X-OH and H₂O species. Most of these potential issues, however, can be easily dismissed with care in setting up the NMR experiment.

In all NMR studies of hydrated NaAlSi₃O₈ glasses (Eckert et al., 1988, Kohn et al., 1989, Zavelisky et al., 1999, Schmidt et al., 2001, and the present studies) the spectrometers employed all provide sufficient RF power and fast digitizers to excite and collect the NMR emission signal, respectively, without distortion. In all of the wide line (static) NMR experiments (Eckert et al., 1988, Zavelisky et al., 1999, Schmidt et al., 2001), specially designed RF probes are employed to minimize receiver delays. This is particularly important with a chemical system where one spin species provides a narrow frequency range signal (long time decay, e.g. X-OH) and another spin species yields a wide frequency range signal (short time decay, e.g. H₂O). Obviously, if the receiver delay time is too long then the widest frequency component, that decays the fastest, will be under-represented relative in the computed species abundance (which would be in all cases H₂O- due to dipolar coupling). The wide line NMR ¹H NMR experiments would be most susceptible to such an effect, but the data of Eckert et al. (1988), Zavelisky et al. (1999), Riemer et al. (2001) and Schmidt et al. (2001) all reveal considerable H₂O content with total water content and complete care in regards to the issues associated with wide line NMR. With 8 kHz MAS (Eckert et al., 1988) and 22 kHz MAS (this study) these requirements are reduced enormously and are easily met by the respective NMR spectrometers. So the remaining potential issues, regarding avoiding non-representative spectra, would have to be with internal issues related to the spin species themselves.

All pulsed NMR experiments signal average over a number of acquisitions (typically 100's to many 1000's). An important experimental parameter is the recycle delay (RD) that allows the nuclear spin system to relax back to thermal equilibrium. This relaxation is exponential and governed by a rate constant $(1/T_1)$. For pulse nutation angles of 90°, the recycle delay (the time between acquisitions) must be greater than $5 \times T_1$ (Ernst et al., 1991), if the RD is too short then signal will be lost through "longitudinal saturation". Provided that all spins have the same value of T_1 , no spectral distortion will occur. In the case of H speciation in hydrous glasses, H₂O species might have a shorter T₁ than isolated X-OH due to enhanced relaxation through dipolar coupling, so there is a potential to artificially enhance "H2O" signal over "X-OH" signal if RD values are too short. The potential for so-called "T₁ effects" has been accounted for in all five of the NMR studies using ¹H NMR of hydrous NaAlSi₃O₈ glasses (Eckert et al., 1988, Kohn et al., 1989, Zavelisky et al., 1999, Schmidt et al., 2001, and the present study). Furthermore, for NaAlSi₃O₈ glasses there are abundant ²³Na and ²⁷Al

nuclei whose magnetic interactions with ¹H will aid in the reduction of T₁. The potential of "T₁ effects" leading to spectral distortion in any of the aforementioned ¹H NMR studies on hydrous NaAlSi₃O₈ glasses is ruled out.

Excluding the above as sources of ¹H NMR spectral distortion, we then have to focus on whether our assumption that dipolar coupling primarily (exclusively) identifies H₂O species over X-OH species. As shown in Fig. 9, dipolar coupling between a pair of protons only becomes significant only at distances less than 2.5 Å (approximately the distance of ¹H's in a Si-(OH) Q² species). If there exists dense water clustering, closely proximal X-OH's and H₂O's could all be subjected dipolar coupling and, thus, would contribute to the sideband intensity beyond what isolated "H₂O" molecules provide (Figs. 4 and 5). Robert et al. (2001) directly set out to detect multiple quantum signals associated with such clustering and were only able to efficiently generate double-quantum coherences (due to H₂O) and detected a weak 4-quantum signal (plausibly due to rare H₂O pairs). No other multiple quantum coherences were detected. They concluded that at least up to 3.2 wt% total water, evidence for dense H-clustering was not observed. Presumably the probability of H clustering would increase with total water content. In the present case of hydrous NaAlSi₃O₈ glasses, side band intensity relative to the center band begins to decrease at 4 wt% total water and decreases continuously up to 10 wt% (Fig. 4). This trend is the opposite of what would be expected if dense H clustering occurred with increasing total water content because that would increase side band intensity.

It should be noted that in the case of hydrous glasses with large NBO/T(initial), e.g. CaMgSi₂O₆ compositions (NBO/T = 2), there is an additional solution mechanism that forms M(OH)₂ (Ca²⁺, Mg²⁺) species (Xue and Kanzaki, 2004). Subsequent work showed that the ¹H in the M(OH)₂ species are dipolar coupled through close proximity (Xue and Kanzaki, 2008). This means for such high NBO/T glasses, some OH species [as Mg(OH)₂] will also contribute to spinning side band intensity. This is not evident in low NBO/T aluminosilicate systems, e.g. NaAlSi₃O₈ and in the case of hydrous CaAl₂Si₂O₈ glasses no M(OH)₂ species are detected (Xue and Kanzaki, 2008).

The only remaining means of explaining the reduction in sideband intensity with increased total water content and, thus, reconciling the NIR and ¹H MAS NMR data, would be to assume that by some mechanism, some fraction of H₂O molecule's intramolecular dipolar coupling was substantially reduced with increased total water content. This could arise if, with increasing total water content, some H₂O molecules became significantly more mobile, thus reducing ¹H-¹H dipolar coupling. There is, however, no evidence of such enhanced H₂O mobility with increasing water content in any of the static studies of hydrous NaAlSi₃O₈ composition glasses (Eckert et al., 1988, Zavelisky et al., 1999, Riemer et al., 2001, and Schmidt et al., 2001).

The analysis above leads to the conclusion that there is no hidden problem in the ¹H MAS NMR experiments that can account for the disparity in what is observed for hydrous NaAlSi₃O₈ glasses via NIR (Figs. 1 and 2) and the ¹H MAS NMR spectroscopies (Figs. 3 and 4). There

is, therefore, a genuine and significant discrepancy between X-OH and H₂O speciation as determined by NIR and ¹H NMR, respectively, in the present study.

It is then particularly surprising that an earlier ¹H (static) NMR study of water speciation in variously hydrated NaAlSi₃O₈ glasses by Schmidt et al (2001), that also exploits the physics of dipolar coupling to distinguish H₂O from X-OH, determined H speciation with total water content that largely mimics what their NIR data (and the present NIR data, Figs. 1 and 2) suggests. Schmidt et al's (2001) study of hydrous NaAlSi₃O₈ glasses over a similar range of total water contents record vastly differing magnitudes in dipolar coupling interactions (hence determined X-OH and H₂O speciation) as compared with the present data. There are three other ¹H NMR studies of hydrous NaAlSi₃O₈ glasses (Eckert et al., 1988, Kohn et al., 1989, Zavelisky et al., 1999) that exhibit differences in water speciation with total water content in comparison to what is reported in the present study and with that previously by Schmidt et al. (2001).

Each of the ¹H NMR studies of hydrated NaAlSi₃O₈ melts (Eckert et al., 1988, Kohn et al., 1989, Zavelisky et al., 1999, Schmidt et al., 2001, and the present study) employed different ¹H NMR experiments (i.e., static at low T and 4, 8, and 22 kHz MAS at room T) and the resultant ¹H NMR spectra are different even as the relevant effects on all the spectra are all due to dipolar coupling. These differences in NMR methods make direct comparison of the different spectra difficult. Furthermore, neither Kohn et al. (1989) nor Zavelisky et al. (1999) extracted quantitative water speciation from their respective ¹H NMR spectra.

In order to derive a common reference frame for comparison, we convert all of the earlier ¹H NMR data for water in hydrous NaAlSi₃O₈ glasses into theoretical ΣSB (1)/CB ratios (assuming that only H₂O contributes to side band intensity). In other words, this is as if all studies used equivalent conditions of 22 kHz MAS ¹H NMR. Zavelisky et al. (1999) did not fit their ¹H NMR spectra to obtain X-OH and H₂O speciation data. In order to obtain these data from their spectra, the fitted wide line data of Riemer et al. (2001) and Schmidt et al. (2001) was used to calibrate a fit of the wide line ¹H NMR spectra of Zavelisky et al. (1999) to retrieve X-OH and H₂O speciation from the earlier study. Eckert et al. (1988) used the dipolar coupling strength observed for analcite as opposed to actual dipolar coupling strength of H₂O in NaAlSi₃O₈ glass (see discussions above) which leads to an underestimate for the amount of molecular water present. We correct their speciation estimates to account for the weaker dipolar coupling associated with H₂O in hydrous NaAlSi₃O₈ glass. Kohn et al (1989) only presented a single ¹H MAS NMR spectrum of hydrous NaAlSi₃O₈ glass (8.2 wt% total water) acquired at a MAS frequency of 4 kHz and room temperature and did not use their spectrum to make any estimate of water speciation. Simulating the ¹H MAS NMR spectrum of molecular water at 4 KHz MAS with dipolar coupling equal to 22.8 KHz makes it possible to determine the speciation from Kohn et al.s (1989) data and determine a theoretical value for $\Sigma SB(1)/CB$ at 22 kHz MAS.

These theoretically derived $\Sigma SB(1)/CB$ ratios for hydrous NaAlSi₃O₈ glasses (Eckert et al., 1988, Kohn et al., 1989, Zavelisky et al., 1999, Schmidt et al., 2001) and current experimental values are plotted against total water content (wt %) in Fig. 15. Clearly the ¹H NMR (static and MAS) data for hydrous NaAlSi₃O₈ glasses over similar ranges in total water content vary greatly across the total water concentration range. At low total water contents (<4 wt%), the trends for the data of Eckert et al. (1988), Zavelisky et al. (1999), Schmidt et al. (2001) and the present data are somewhat similar in that all the data trend towards greater molecular H₂O speciation with total water content. although each data set exhibits differences in the concentration of molecular H₂O species across a similar range of water compositions. Above a total water content of 4 wt % one observes significant differences in the trends in water speciation with increasing total water content in the various studies. The present data and that of Eckert et al. (1988) and Kohn et al. (1989) indicate that H₂O speciation begins to drop significantly as total water content increases, whereas the concentration of H₂O species continue to rise in the data of Zavelisky et al. (1999) and Schmidt et al. (2001). As all five experiments discriminate molecular H₂O through dipolar coupling interactions between protons, the comparison in Fig. 15 reveals the strength of this interaction (hence the species abundance of H₂O relative to X-OH) differs from experiment to experiment even though the glass compositions are identical.

For all of ¹H NMR experiments performed on hydrous NaAlSi₃O₈ glasses there are no concerns about any experimental considerations in any of these analyses that could give rise to spurious estimates of X-OH and H₂O speciation. Therefore, the dissimilarity in the extent of dipolar coupling interactions and, thus the concentration of molecular H₂O (Fig. 15) revealed in different studies is real. This leads to the only other experimental variable, not yet considered, which is how each hydrous glass synthesis experiment was performed. The hydrous NaAlSi₃O₈ glasses in the present experiment were synthesized as melts at 1400 °C in a piston cylinder apparatus at 1.5 GPa, cutting current to the furnace assembly induces quenching to glasses at a rate of 100-200 °c/sec. Eckert et al. (1988) also used a piston cylinder apparatus with temperature 1400– 1450 °C and pressures ranging from 1.5 to 2.0 GPa followed by isobaric quench at a rate of 100-200 °C/sec. Kohn et al (1989) also used a piston cylinder apparatus at P = 1.0 GPa, T = 1100 °C where quench rate is assumed to be 100 °C/sec. Schmidt et al. (2001) employed an internally heated pressure vessel (IHPV), heating to 1200 °C and a pressure of 0.5 GPa followed by isobaric quench at a rate of 100 °C/min. Zavelisky et al. (1999) also used an IHPV, the T ranging from 1250 to 1100 °C, and spanning three water contents (3, 6, and 8 wt%). Pressures employed were 0.05 GPa (3 wt%), 0.2 GPa (6 wt%), and 0.5 GPa (8 wt %). After melt synthesis each run was quenched isobarically at a rate of 100 °C/min.

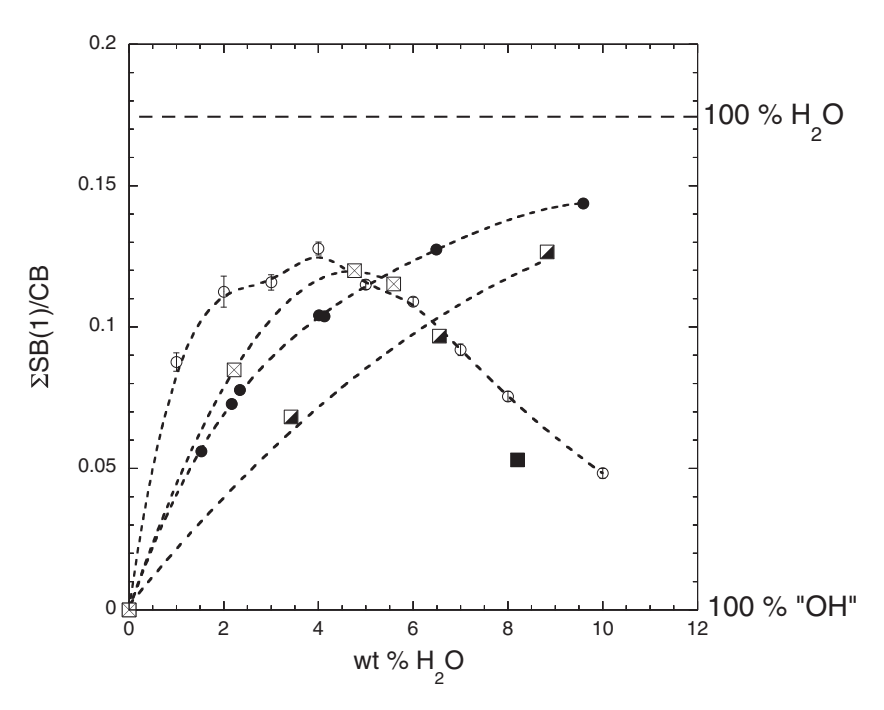


Fig. 15. A comparison of side band (SB) to center band (CB) ratios ($\Sigma SB(1)/CB$) for hydrous NaAlSi₃O₈ glasses (open circle, this study) with simulated $\Sigma SB(1)/CB$ (assuming ¹H MAS NMR, $\omega_r/2\pi = 22$ kHz) derived from H₂O and X-OH speciation from previous studies of hydrous NaAlSi₃O₈ glasses using static ¹H NMR (closed circle, Schmidt et al., 2001), static ¹H NMR (half-closed square, Zavelisky et al., 1999), ¹H MAS NMR ($\omega_r/2\pi = 8$ kHz) (crossed boxes, Eckert et al., 1988), and ¹H MAS NMR ($\omega_r/2\pi = 4$ kHz)(black square, Kohn et al., 1989). The bold dashed line at 0.175 delineates 100 % H₂O species. Although the five glass compositions are the same and span the same total water content range, the five different experiments report differences in the extent of dipolar coupling with total water content on, hence, differences in X-OH and H₂O speciation in the hydrous NaAlSi₃O₈ glasses.

Two potentially significant differences exist amongst the five different studies of hydrous NaAlSi₃O₈ glass synthesis. First there is a nearly two order of magnitude slower quench rate using a IHPV than with a piston cylinder apparatus (it is noted that when an IHPV is used vertically with the sample suspended on a fusible wire, very rapid quenching is possible, e.g. Malfait and Xue (2010), however in the studies of Zavelisky et al. (1999), Riemer et al. (2001), and Schmidt et al. (2001) such rapid quench methods were not employed). Second, at lower water contents the synthesis pressures in the various studies range from 0.05 to 1.5 GPa.

It is worth considering whether these differences could explain the significant variation observed in Fig. 15. Focusing on the potential effect of significantly different quench rates first, 30 years ago (Stolper, 1989) reported that the glass transition temperature (T_g) of melts should be inversely related to water content. Shortly thereafter, Dingwell and Webb (1990) further explained that glass transition temperature must be quench-rate dependent, where T_g increases with quench rate. They went further to conclude that quench studies of X-OH and H_2O speciation in hydrous glasses over ranges of water composition (as is the case here and elsewhere) cannot, therefore, be considered isothermal studies as T_g must change with water content.

It is widely accepted that the equilibrium described in Eq. (1) should shift to the right with increased temperature (making X-OH with increased T) and with cooling shift to the left (making H₂O at lower T). Thus, the expectation is that if X-OH and H₂O speciation is set at the glass transition, then speciation will be a function of both quench rate and total water content (Dingwell and Webb, 1990). Experiments using an IHPV, quenching slowly (lower Tg), should be expected to yield higher concentrations of H₂O (at highest total water content) and experiments using a piston cylinder apparatus, quenching faster (higher T_g), should be expected to yield a higher concentration of X-OH (at highest total water content) as glasses, detected via ¹H NMR. At the highest total water contents, this is what is observed comparing the magnitude of dipolar coupling observed for Zavelisky et al. (1999) Schmidt et al. (2001) (using IHPVs) and with what is observed with the present data and the one data point of Kohn et al. (1989) (using a piston cylinder apparatus) Fig. 15. It is, therefore, plausible that the very large differences in H₂O content observed in comparison of the experiments of Zavelisky et al. (1999) and Schmidt et al. (2001) with the present data (Figs. 4 and 12) and the one data point of Kohn et al. (1989) is the result of re-equilibration (partial or total?) at a lower T_g with the slower quench (IHPV).

While quench effects may explain the disparity amongst the various experiments (Fig. 15) in the ¹H NMR results at high total water contents, quench effects may not explain why, at low total water contents, the current ¹H MAS NMR data reveal such strong dipolar interactions (high H₂O contents) relative to what other ¹H NMR experiments report (Eckert et al., 1988, Zavelisky et al., 1999, and Schmidt et al., 2001). The principal difference between the four experiments (aside from quench rate) at low total water contents is synthesis pressure. Our experiments were

performed at 1.5 GPa across the range of water contents at lower water contents, while the experiments of Zavelisky et al. (1999) and Schmidt et al. (2001) were performed a lower pressures (0.05 and 0.5 GPa, respectively). What is observed, Fig. 15, is that for the lower pressure experiments, at low total water contents, there is much weaker dipolar coupling (lower H₂O) observed. This may suggest, an apparent relationship between pressure (1.5, 0.5 and 0.05 GPa) and H₂O species abundance, where the abundance of H₂O species increases with higher pressure at a constant total water content. If pressure is the cause for the increased H₂O content at low total water concentration. then this could suggest that there is significant positive ΔV contribution when moving the equilibrium to the right as described by Eq. (1). Such a potential relationship between P and water speciation at low H₂O content will need to be explored experimentally. If one accepts the issues regarding quenching and speciation as a function of water content (Dingwell and Webb, 1990) and the possible effect of pressure on H₂O content via Eq. (1) (observed at lower water content); then these two factors alone may be sufficient to explain the disparity presented amongst the data presented in Fig. 15.

5. GEOCHEMICAL IMPLICATIONS

Whether H₂O operates as a network modifying oxide (e.g. Na₂O) or as a neutral constituent (e.g. Ne or Ar) is the crux of the question about how water controls melt properties. The addition of alkali oxide (e.g. Na₂O) to SiO₂ has a profound effect on the reduction of melt viscosity (Urbain et al., 1982, Knoche et al., 1994). Sodium oxide is a very strong network modifier, meaning that every Na₂O added per silica tetrahedron results in the formation of 2 NBO's (Maekawa et al., 1991). It is interesting then, therefore, to compare the changes in NBO/T with H₂O addition with that derived from Na₂O. In Fig. 16 the value of NBO/ T derived from Na₂O and H₂O addition are compared, the latter being derived from the present study through ¹H NMR and previous NIR (Silver and Stolper, 1989) data. The NIR results (Silver and Stolper, 1989 and many others) suggest only a minor increase in NBO/T, approximately from NBO/T = 0 (0 % H_2O) up to the level of an average phonolite (NBO/T = 0.15, Mysen, 2014). The ${}^{1}H$ NMR results, on the other hand indicate at 29 mole % water (determined on a single tetrahedron, T = 1, basis based on 10 wt% total H₂O) achieves a value of NBO/T that approaches that of an average tholeiite (NBO/T = 0.8, Mysen, 2014). Thus, the ¹H NMR speciation results support the idea that the reduction viscosity in hydrous NaAlSi₃O₈ melt (e.g. Nowak and Behrens, 1997, Whittingston et al., 2001 and others) would be due to continuous network depolymerization. Whereas the NIR results (e.g. Silver and Stolper, 1989) suggest that depolymerization ceases at ~ 4 wt% H_2O (~ 13 mol % H_2O) (Fig. 16). If the NIR data were accurately reporting "OH" content, hence the extent of depolymerization, then this would require that any subsequent reductions in viscosity (beyond ~4 wt%) would require that water provides a

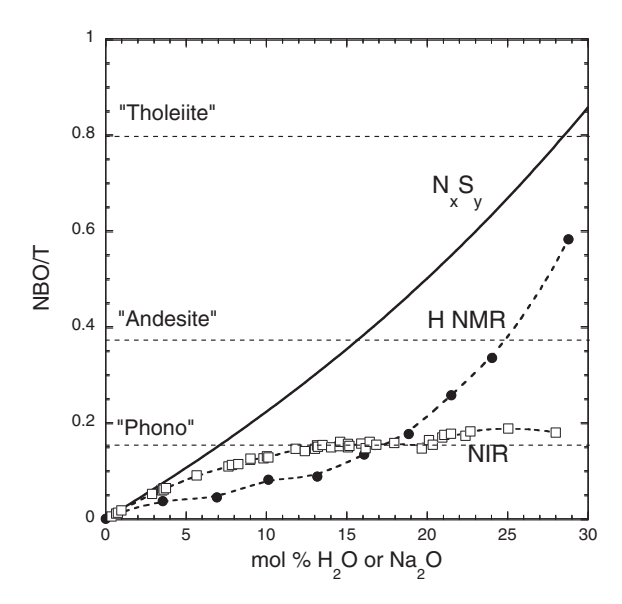


Fig. 16. A plot of NBO/T as a function of mol % H₂O or Na₂O (determined for a single tetrahedral formula, e.g. Na_{0.25}Al_{0.25}Si_{0.75}-O₂). Sodium silicate glasses (NxSy) represent the maximum degree of depolymerization that at \sim 30 mol % Na₂O exceed that of mean tholeite composition. The dependence of NBO/T for hydrous NaAlSi₃O₈ glasses are presented derived from 1 H NMR (solid circles, this study) and NIR spectroscopy (open squares, from Silver and Stolper, 1989). Mean NBO/T for anhydrous phonolite composition ("Phono"), andesite ("Andesite"), and tholeite ("tholeite") are shown with dashed lines.

viscosity reduction mechanism other than network depolymerization.

In most, if not all, models that aim to predict the effect of water on melt viscosity (e.g. Vetere et al., 2006, Whittingston et al., 2001), a purely empirical approach is employed where the explicit role of water speciation is not considered, rather only the effect of total water content is considered. The same is true in the case of modeling of the effect of water on melt resistivity, where water is considered only in terms of total water content in empirical models with fitted adjustable coefficients (e.g. Guo et al., 2016). In the case of water diffusivity, Nowak and Behrens (1997) also formulated a functional empirical equation for the effect of water on water diffusivity using only the total concentration of water as a parameter and including adjustable and fitted constants where no specific consideration of speciation (eg. 1) was included.

The role of water speciation has been more explicitly considered in other studies that aim to model water diffusivity in melts as a function of water content. As is the case with the change in viscosity and resistivity with increased H₂O, the apparent diffusion coefficient of water also exhibits an exponential increase with increased water content (e.g. Zhang et al., 1991, Behrens and Nowak, 1997, Nowak and Behrens, 1997). Infrared spectro-microscopy is the best way to measure H₂O diffusion profiles in either dehydration studies or diffusion couple studies, thus also affording measurement of the NIR combination bands that are attributed to X-OH and H₂O (see many reference above).

As it is universally agreed that water in melts and hydrous glasses exists as both Si, Al-OH and H₂O [acknowledging that with peralkaline compositions with high initial NBO/T some $M(OH)_{1-2}$ (M = alkali and alkali earth cations) speciation may also occur, e.g. Xue and Kanzaki, 2004, Cody et al., 2005]. Focusing on alumino-silicate compositions, Zhang et al. (1991) recognized that there would necessarily be two diffusion constants to consider, DOH and D_{H2O} . Zhang et al. (1991) concluded that $D_{OH} \ll$ D_{H2O}, such that water diffusivity was controlled exclusively by D_{H2O}. To account for the increased diffusivity with increasing water content led Zhang et al. (1991) to propose that D_{H2O} exhibits an exponential relationship with X_{H2O} (derived from NIR data) that when combined with some adjustable coefficients allows faithful modeling of water diffusivity with both water content and temperature. This approach has been successfully applied by others with minor variations (e.g. Ni et al., 2009, 2013) to quantitatively model water diffusivity in hydrous silicate glasses.

The general consensus was that Si,Al-OH bound water can only diffuse by first combining with another Si,Al-OH species to form molecular water (e.g. Tomozawa, 1985). This view was challenged in an analysis by Behrens and Nowak (1997) who presented an additional mechanism by which isolated Si.Al-OH groups ("singletons"), in melts, could diffuse without recombination to form H₂O. In light of the vastly different assessment of water speciation, based on ¹H NMR outlined in the text above, wherein the proportion of Si,Al-OH species increases and exceeds molecular H₂O at the highest water concentrations, it appears Si,Al-OH species diffusion, either as pairs or "singletons", must be much more influential at high water contents than previously considered. The fact that ¹H NMR data indicates that at low total water content (Fig. 12) molecular H₂O abundance is \sim equal to that of Si,Al-OH (as H₂O) provides some solution to the apparent bottleneck to diffusivity at very low water content, where NIR speciation suggests water speciation exists at nearly exclusively Si, Al-OH, that provides no simple means of dehydration if H₂O speciation is required for water diffusion in glasses (Ni et al., 2013).

The present data suggest that the primary effect of water addition is due to a reduction in NBO/T, meaning that to a large extent water operates as a "network modifier", continuously with increased water addition. Ultimately, any study that attempts to derive mechanistic understanding relying specifically on the role of water speciation on melt properties (e.g. viscosity, resistivity, diffusivity, or others) derived from NIR combination bands, should be reassessed in light of the present ¹H NMR results. This said, all previous studies that model melt properties as a function of total water content, empirically and without regard to speciation, are unaffected by the discrepancy in water speciation between ¹H NMR and NIR spectroscopies.

6. CONCLUSIONS

For nearly 40 years it has been shown that NIR spectroscopy reliably and systematically responds to variation in total water content and can certainly be reliable to quantitatively ascertain total water content in hydrous glasses.

In fact, use of the 4500 and 5200 cm⁻¹ bands may provide the easiest means of determining water content because of the highly consistent trends in intensity with total water content (e.g., Silver et al., 1990). However, the use of the 4500 and 5200 cm⁻¹ bands, specifically, for the purpose of establishing X-OH and H₂O speciation is in our opinion not supported by previous and present ¹H NMR data. Variation in dipolar coupling observed in ¹H NMR data from various hydrous NaAlSi₃O₈ glasses that is expected to reflect the concentration of molecular water is not simultaneously observed in variation in the 4500 and 5200 cm⁻¹ bands in the NIR spectra from the same glasses of the same composition.

The ¹H NMR data faithfully record H₂O species content (and X-OH by difference) through dipolar coupling strength. However, what one observes is that speciation is a complex function of how the glasses are synthesized, quench rate, in particular, being very significant at higher water contents. In the present case the limited D and ²⁹Si MAS NMR spectra lead to conclusions that are internally consistent with those derived from ¹H MAS NMR data, suggesting that for the current experiments there is progressive depolymerization (hence increased X-OH formation with increased total water content).

The fact that the static ¹H NMR data of Schmidt et al., 2001 and the present ¹H MAS NMR data lead to completely different water speciation assessments, even while NIR spectroscopy of hydrous NaAlSi₃O₈ glasses in both experiments lead to identical speciation assessments means that ¹H NMR data cannot be used to re-calibrate the NIR results as was proposed and done by Yamashita et al. (2008). The most reasonable conclusion is that the intensities of the 4500 and 5200 cm⁻¹ bands do not faithfully report X-OH and H₂O species concentrations in hydrous alumino-silicate glasses and there does not appear to be any solution that would approve the use of NIR spectroscopy for X-OH and H₂O speciation determination.

Moving forward, it appears that ¹H NMR, either static or using MAS methods, does faithfully record X-OH and H₂O speciation and should be the primary method making such a determination. This said, as discussed above and previously by others (e.g. Dingwell and Webb, 1990), how hydrous glasses are synthesized likely plays an enormous role on the final (at the glass transition temperature, T_g) speciation. Therefore, accurate determination of speciation does not automatically reveal clearly resolvable thermodynamics (e.g. Eq. (1)). Rather, re-equilibration kinetics (during quenching) particularly at higher total water contents adds an additional layer of complexity. It appears likely that many experiments will need to be performed on hydrous glasses employing the widest range of controllable experimental parameters (e.g. total water content, quench rates and pressure) in order to sort out exactly the details of water-silicate melt interactions to a satisfactory level and it is recognized that there are limits to what can be done experimentally (e.g., upper limits on quench rates). Furthermore, as noted by Eckert et al. (1988), the presence of iron presents an additional and significant issue in the application of ¹H NMR for the purpose of determining water speciation in natural (iron bearing) glasses.

Finally, while NIR spectroscopy can be performed at temperatures above the glass transition into the silicate melt phase, ¹H NMR will fail to provide any information about water speciation at high temperatures. Such experiments would be extremely difficult and to the best of our knowledge high temperature NMR studies of volatile containing melts have never been done. Even if it could be done, the molecular dynamics of X-OH and H₂O at high temperatures are such that dipolar coupling will no longer be available to distinguish the two species. This means that the thermodynamics and kinetics governing water speciation will need to be understood very well at lower temperatures, in the glassy-solid state, such that extrapolation might be made to magmatic temperatures. It remains to be seen whether this is possible.

Declaration of Competing Interest

The authors declare that they have no known competing financial interests or personal relationships that could have appeared to influence the work reported in this paper.

ACKNOWLEDGMENTS

We gratefully appreciate the suggestions by the Associate Editor Dr. Wim van Westrenen and the anonymous reviewers that helped improve the clarity of the manuscript. We gratefully appreciate discussions with Drs. Zack Gaballe, Nico Keuter and Mike Walter and other colleagues whose suggestions and insights improved the text. We gratefully thank the authors of the SIMPSON code for making this program available to the NMR community. We gratefully thank the Smithsonian Institution, Department of Mineralogy, for providing well characterized samples of analcite and natrolite. We gratefully acknowledge the W. M. Keck foundation, the National Science Foundation and the Carnegie Institution for support of the W. M. Keck Solid State NMR and the FTIR facilities. DF and BOM gratefully acknowledge support by the NSF (EAR 1761388).

APPENDIX A. SUPPLEMENTARY MATERIAL

Supplementary data to this article can be found online at https://doi.org/10.1016/j.gca.2020.07.011.

REFERENCES

Abragam A. (1961) *The Principles of Nuclear Magnetism*. Clarendon Press, Oxford, p. 599p.

Acocella J., Tomozawa M. and Watson E. B. (1984) The nature of dissolved water in sodium silicate glasses and its effect on various properties. J. Noncrystal. Solid. 65, 355–372.

Bak M., Rasmussen J. T. and Nielsen N. C. (2000) SIMPSON: A general simulation program for solid-state NMR spectroscopy. J. Magn. Resonance 147, 296–330.

Bartholomew R. F., Butler B. L., Hoover H. L. and Wu C. K. (1980) Infrared spectra of a water-containing glass. *J. Amer. Ceram. Soc.* **63**, 481–485.

- Bartholomew R. F. and Schreurs J. W. H. (1980) Wide-line NMR study of protons in hydrosilicate glasses of different water content. J. Non-Cryst. Solids. 39, 679–684.
- Behrens H. and Nowak M. (1997) The mechanisms of water diffusion in polymerized silicate melts. *Contrib. Mineral. Petrol.* 126, 377–385.
- Behrens H., Romano C., Nowak M., Holtz F. and Dingwell D. B. (1996) Near-infrared spectroscopic determination of water species in glasses of the system MAlSi₃O₈ (M=Li, Na, K): an interlaboratory study. *Chem. Geol.* **128**, 41–63.
- Boyd and England (1960) The quartz-coesite transition. J. Geophys. Res. 65, 749–756.
- Burnham C. W. (1963) Viscosity of a water-rich pegmatite melt at high pressure. *Geol. Soc. Am. Spec. Paper* **76**, 26.
- Carrol M. R. and Stolper E. M. (1993) Noble gas solubilities in silicate melts and glasses: New experimental results for Argon and the relationship between solubility and ionic porosity. *Geochim. Cosmochim. Acta* 57, 5039–5051.
- Cherikova N. and Yamashita S. (2015) In situ spectroscopic study of water speciation in the depolymerized Na₂Si₂O₅ melt. *Chem. Geol.* **409**, 149–156.
- Cody G. D., Bysen B. O. and Lee S. K. (2005) Structure vs. composition: a solid-state ¹H and ²⁹Si NMR study of quenched glasses along the Na₂0-SiO₂-H₂O join. *Geochim. Cosmochim. Acta* **69**, 2373–2384.
- Dingwell D. B. and Webb S. L. (1990) Relaxation in silicate melts. *Eur. J. Mineral.* **2**, 427–449.
- Dixon J. A., Stolper E. M. and Holloway J. R. (1995) An experimental study of water and carbon dioxide solubilities in mid-oceanic ridge basaltic liquids: Calibration and solubility models. J. Petrol. 36, 1607–1631.
- Dodd D. M. and Fraser D. B. (1966) Optical determination of OH in fused silica. *J. Appl. Phys.* **37**, 3911.
- Eckert H., Yesinowski J. P., Stolper E., Stanton T. R. and Holloway J. (1987) The state of water in rhyolitic glasses: a deuterium NMR study. *J. Non-Cryst. Solids.* **93**, 93–114.
- Eckert H., Yesinowski J. P., Silver L. A. and Stolper E. (1988) Water in silicate glasses: quantitation and structural studies by ¹H solid echo and MAS-NMR methods. *J. Phys. Chem.* **92**, 2055–2064.
- Ernst R. R., Bodanhausen G. and Wokuan A. (1991) *Principles of Nuclear Magnetic Resonance in one and two dimensions*. Clarendon Press, Oxford, p. 610p.
- Giordano D. and Dingwell D. B. (2003) Non-Arrhenian multcomponent melt viscosity a model. *Earth. Planet. Sci. Lett.* 208, 337–349.
- Guo X., Zhang L., Behrens H. and Ni H. (2016) Probing the status of felsic magma reservoirs: constraints from the P-T-H₂O dependence on electrical conductivity of rhyolitic melt. *Earth. Planet. Sci. Lett.* **433**, 54–62.
- Hammer V. M. F., Libowisky E. and Rossman G. R. (1998) Single-crystal IR spectroscopy of very strong hydrogen bonds in pectolite NaCa₂[Si₃O₈(OH)] and serandite NaMn₂[Si₃O₈(OH)]. *Am. Mineral.* **83**, 569–576.
- Harris D. C. and Bertolucci M. D. (1978) Symmetry and Spectroscopy, an introduction to vibrational and electronic spectroscopy. Oxford University Press, New York, p. 550p.
- Herzfeld J. and Berger A. E. (1980) Side band intensities in NMR spectra of samples spinning at the magic angle. *J. Chem. Phys.* **73**, 6021–6030.
- Knoche R., Dingwell D. B., Seifert F. A. and Webb S. L. (1994) Nonlinear properties of supercooled liquids in the system Na₂O-SiO₂. Chem. Geol. 116, 1–16.
- Kohn S. C., Dupree R. and Smith M. E. (1989) A multi-nuclear magnetic resonance study of the structure of hydrous NaAlSi₃-O₈ glasses. *Geochim. Cosmochim. Acta* 53, 2925–2935.

- Kummerlen J., Merwin L. H., Sebald A. and Keppler H. (1992) Structural role of H₂O in sodium silicate glasses: results from ²⁹Si and ¹H NMR spectroscopy. *J. Phys. Chem.* **96**, 6405–6410.
- Kushiro I. (1976) Change in viscosity and structure of melt of NaAlSi2O6 composition at high pressures. J. Geophys. Res. 81, 6347–6350.
- Kushiro I. and Mysen B. O. (2002) Possible effect of melt structure on the Mg-Fe²⁺ partioning between olivine and melt. *Geochim. Cosmochim. Acta* **66**, 2267–2273.
- Lee S. K. and Stebbins J. F. (1999) The degree of aluminum avoidance in aluminosilicate glasses. *Am. Min.* **84**, 937–945.
- Le Losq C., Cody G. D. and Mysen B. O. (2015a) Complex IR spectra of OH groups in silicate glasses: Implications for the use of the 4500 cm⁻¹ IR peak as a marker of OH- groups concentration. *Am. Mineral.* **100**, 945–950.
- Le Losq C., Mysen B. O. and Cody G. D. (2015b) Water and magmas: insights about the water solution mechanisms in alkali silicate melts from infrared, Raman, and ²⁹Si solid-state NMR spectroscopies. *Prog. Earth. Planet. Sci.* **2**, 1–16.
- Le Losq C., Mysen B. O. and Cody G. D. (2016) Intramolecular fractionation of hydrogen isotopes in silicate quenched melts. *Geochem. Perps. Lett.* **2**, 87–94.
- Levine I. N. (1975) Molecular Spectroscopy. John Wiley and Sons, New York, p. 491p.
- Levitt M. H. (2009) Spin Dynamics-Basics of Nuclear Magnetic Resonance. John Wiley and Sons, Chichester UK, p. 714p.
- Libowitsky E. (1999) Correlation of O-H stretching frequencies and O-H···H bond lengths in minerals. *Mon. für Chemie* **130**, 1047–1059
- Lippma E., Mägi S. A., Englehardt G. and Grimmer A.-R. (1980) Structural studies by Solid-State High Resolution ²⁹Si NMR. *J. Am. Chem. Soc.* **102**, 4889–4893.
- Lippma E., Mägi M., Samoson A., Tarmak M. and Engelhardt G. (1981) Investigation of the structure of zeolites by solid-state high resolution ²⁹Si NMR spectroscopy. J. Am. Chem. Soc. 103, 4992–4996.
- Maekawa H., Maekawa T., Kawamura K. and Yokokawa T. (1991) The structural groups of alkali silicate glasses determined by ²⁹Si MAS-NMR. *J. Non-Chryst. Solids.* 127, 53–64.
- Malfait W. J. and Xue X. (2010) The nature of hydroxyl groups in aluminosilicate glasses: quantifying Si-OH and Al-OH abundances along the SiO₂-NaAlSiO₄ join by ¹H, ²⁷Al-¹H and ²⁹Si-¹H NMR spectroscopy. *Geochim. Cosmochim. Acta* 74, 719–737.
- Mandeville C. W., Webster J. D., Rutherford M. J., Taylor B. E., Timbal A. and Faure K. (2002) Determination of molar absorptivities for infrared bands of H₂O in andesite glasses. Am. Min. 87, 813–821.
- Mauri F., Pasquarello A., Pfrommer B. G., Yoon Y.-G. and Louie S. G. (2000) Si-O-Si bond-angle distribution in vitreous silica from first principles ²⁹Si NMR analysis. *Phys. Rev. B* **62**, R4786.
- Mehring M. (1976) High Resolution NMR Spectroscopy in Solids. Springer-Verlag, Berlin, p. 246p.
- Mysen B. O. (2007) Olivine/Melt transition metal partitioning, melt compositions, and metal structure- influence of Al³⁺ for Si⁴⁺ substitution in the tetrahedral network of silicate melts. *Geochim. Cosmochim. Acta* 71, 5500–5513.
- Mysen B. O. (2014) Water-melt interaction in hydrous magmatic systems at high temperature and pressure. *Prog. Ear. Planet. Sci.* 1, 1–18.
- Mysen B. O. and Richet P. (2019) *Silicate Glasses and Melts*. Elsevier, Cambridge US, p. 708p.
- Newman S., Stolper E. M. and Epstein S. (1986) Measurement of water in rhyolitic glasses: Calibration of an infrared spectroscopic technique. Am. Min. 71, 1527–1541.

- Ni H., Keppler H., Manthilake M. A. G. M. and Katsura T. (2011) Electrical conductivity of dry and hydrous NaAlSi3O8 glasses and liquids at high pressures. *Contrib. Mineral. Petrol.* 162, 501–513.
- Ni H., Liu Y., Wang L. and Zhang Y. (2009) Water speciation and diffusion in haploandesitic melts at 743–873 K and 100 MPa. *Geochim. Cosmochim. Acta* 73, 3630–3641.
- Ni H., Xu Z. and Zhang Y. (2013) Hydroxyl and molecular H₂O diffusivity in haploandesitic melt. Geochim. Cosmochim. Acta 103, 36–48
- Nowak M. and Behrens H. (1995) The speciation of water in haplogranitic glasses and melts determined by in situ nearinfrared spectroscopy. *Geochim. Cosmochim. Acta* 59, 3445– 3450.
- Nowak M. and Behrens H. (1997) An experimental investigation on diffusion of water in haplogranitic melts. *Contrib. Mineral. Petrol.* 126, 365–376.
- Ohlhorst S., Behrens H. and Holtz F. (2001) Compositional dependence of molar absorptivities of near near-infrared OH-and H₂O bands in rhyolitic to basaltic glasses. *Chem. Geol.* **174**, 5–20.
- Olglesby J. V. and Stebbins J. F. (2000) 29Si CPMAS NMR investigations of silanol-group minerals and hydrous aluminosilicate glasses. Am. Min. 85, 722-731.
- Pake G. E. (1948) Nuclear Resonance Absorption in hydrated crystals: fine structure of the proton line. J. Chem. Phys. 16, 327–336.
- Pedersen B. F. and Semensen D. (1982) Neutron diffraction refinement of the structure of gypsum, CaSO₄·2H₂O. *Acta. Crys.* **B38**, 1074–1077.
- Poe B. T., Romano C., Liebske C., Rubie D. C., Terasaki H., Suzuki A. and Funakoshi K. (2006) High-temperature viscosity measurements of hydrous albite liquid using in-situ falling sphere viscometry at 2.5 GPa. *Chem. Geol.* **229**, 2–9.
- Richet P., Lejueune A.-M., Holtz F. and Roux J. (1996) Water and the viscosity of andesitic melts. Chem. Geol. 128, 185–197.
- Riemer T., Schmidt B., Behrens H. and Dupree R. (2001) H₂O/OH ratio determination in hydrous aluminosilicate glasses by static proton NMR and the effect of chemical shielding anisotropy. *Solid State Nucl. Magn. Reson.* **15**, 201–207.
- Robert E., Whittingham A., Fayon F., Pichavant M. and Massiot D. (2001) Structural characterization of water-bearing silicate and aluminosilicate glasses by high-resolution solid-state NMR. *Chem. Geol.* 174, 291–305.
- Romano C., Poe B. T., Mincione V., Hess K. V., Dingwell D. B. (2001) The viscosity of dry and hydrous XAlSi3O8 (X=Li, Na, K, Ca0.5, Mg0.5).
- Schmidt B., Behrens H., Riemer T., Kappes R. and Dupree R. (2001) Quantitative determination of water speciation in aluminosilicate glasses: a comparative NMR and IR spectroscopic study. *Chem. Geol.* **174**, 195–208.
- Scholtz H. (1960) Zur Frage der Unterscheidung zwishen H2Omolekein und OH-gruppen in Gläsern und mineralen. Naturewissenschften 10, 226–227.
- Shaw H. R. (1963) Obsidian-H₂O viscosities at 1000 and 2000 bars in the temperature range 700–900 °C. *J. Geophys. Res.* **68**, 6337–6343.
- Shen A. and Keppler H. (1995) Infrared spectroscopy of hydrous silicate melts to 1000 °C and 10 kbar: direct observation of H₂O speciation in a diamond-anvil cell. *Am. Mineral.* **80**, 1335–1338.
- Silver L. A., Ihinger P. D. and Stolper E. (1990) The influence of bulk composition on the speciation of water in silicate glasses. *Contr. Min. Pet.* 104, 142–162.

- Silver L. and Stolper E. (1989) Water in albitic glasses. *J. Petrol.* **30**, 667–709.
- Slichter C. P. (1996) *Principles of Magnetic Resonance*. Springer-Verlag, New York, p. 655p.
- Smith J. V. and Blackwell C. S. (1983) Nuclear magnetic resonance of silica polymorphs. *Nature* **303**, 223–225.
- Sowerby J. R. and Keppler H. (1999) Water speciation in rhyolitic melt determined by in-situ infrared spectroscopy. *Am. Mineral.* 84, 1843–1849.
- Stolper E. (1982) Water in silicate glasses: an infrared spectroscopic study. Contr. Min. Petrol. 81, 1–17.
- Stolper E. (1989) Temperature dependence of the speciation of water in rhyolitic melts and glasses. Am. Mineral. 74, 1247– 1257.
- Takata M., Acocella J., Tomozawa M. and Watson E. B. (1981) Effect of water content on electrical conductivity of Na₂O-3SiO₂ glass. J. Am. Ceram. Soc. 64, 719–724.
- Tomozawa M. (1985) Concentration dependence of the diffusion coefficient of water in SiO₂ glass. J. Am. Ceram. Soc. 68, 251– 252.
- Tickle R. E. (1967) The electrical conductance of molten alkali silicates. *Phys. Chem. Glasses* **8**, 101–112.
- Urbain G., Bottinga Y. and Richet P. (1982) Viscosity of liquid silica, silictes, and alumino-silicates. *Geochim. Cosmochim. Acta* 46, 1061–1072.
- Vetere F., Behrens H., Holtz F. and Neuville D. R. (2006) Viscosity of andesitic melts- new experimental data and a revised calculation model. *Chem. Geol.* **228**, 233–245.
- Wang Y., Cody S. X., Foustoukos D., Mysen B. O. and Cody G. D. (2015) Very large intramolecular D-H partitioning in hydrated silicate melts synthesized at upper mantle pressures and temperatures. Am. Mineral. 110, 1182–1189.
- Whittingston A., Richet P., Linard Y. and Holtz F. (2001) The viscosity of hydrous phonolite and trachytes. *Chem. Geol.* 174, 209–223.
- Withers A. C. and Behrens H. (1999) Temperature-induced changes in the NIR spectra of hydrous albitic and rhyolitic glasses between 300 and 100 K. *Phys. Chem. Mineral.* 27, 119–132.
- Wu C.-K. (1980) Nature of incorporated water in hydrated silicate glasses. J. Am. Ceram. Soc. 63, 453–457.
- Xue X. and Kanzaki M. (2004) Dissolution mechanisms of water in depolymerized silicate melts: constituents from ¹H and ²⁹Si NMR spectroscopy and ab initio calculations. *Geochim. Cosmochim. Acta.* 68, 5027–5057.
- Xue X. and Kanzaki M. (2008) Structure of hydrous aluminosilicate glasses along the diopside-anorthite join: A comprehensive one- and two-dimensional ¹H and ²⁷Al study. *Geochim. Cosmochim. Acta* **72**, 2331–2348.
- Yamashita S., Kitamura T. and Kusakabe M. (1997) Infrared spectroscopy of hydrous glasses of arc magma composition. *Geochem. J.* **31**, 169–174.
- Yamashita S., Behrens H., Schmidt B. C. and Rupree R. (2008) Water speciation in sodium silicate glasses based on NIR and NMR spectroscopy. *Chem. Geol.* **256**, 231–241.
- Zarubin D. P. (1999) Infrared spectra of hydrogen bonded hydroxyl groups in silicate glasses. A re-interpretation. *Phys. Chem. Glasses* 40, 184–192.
- Zavelisky V. O., Bezmen N. J. and Zharikov V. A. (1999) Water in NaAlSi₃O₈ glasses: OH-groups, isolated molecules, and clusters. J. Non-cryst. Solids 224, 225–231.
- Zhang Y., Belcher R., Ihinger P. D., Wang L., Xu Z. and Newman S. (1997) New Calibration of infrared measurement of dissolved

water in rhyolitic glasses. *Geochim. Cosmochim. Acta.* **61**, 3089–3100.

Zhang Y., Stolper E. M. and Wasserburg G. J. (1991) Diffusion of water in rhyolitic glass. *Geochim. Cosmochim. Acta.* **55**, 441–456.

Zotov N. and Keppler H. (1998) The influence of water on the structure of hydrous sodium silicate tetrasilicate glasses. *Am. Mineral.* **83**, 823–834.

Associate editor: Wim van Westrenen